Journal Pre-proof

Cyclic Bridged analogs of *iso*CA-4: Design, Synthesis and Biological Evaluation

Shannon Pecnard, Olivier Provot, Hélène Levaique, Jérome Bignon, Laurie Askenatzis, Francois Saller, Delphine Borgel, Sophie Michallet, Marie-Catherine Laisne, Laurence Lafanechère, Mouad Alami, Abdallah Hamze

PII: S0223-5234(20)30845-X

DOI: https://doi.org/10.1016/j.ejmech.2020.112873

Reference: EJMECH 112873

To appear in: *European Journal of Medicinal Chemistry*

Received Date: 21 August 2020

Revised Date: 21 September 2020

Accepted Date: 21 September 2020

Please cite this article as: S. Pecnard, O. Provot, H. Levaique, J. Bignon, L. Askenatzis, F. Saller, D. Borgel, S. Michallet, M.-C. Laisne, L. Lafanechère, M. Alami, A. Hamze, Cyclic Bridged analogs of *iso*CA-4: Design, Synthesis and Biological Evaluation, *European Journal of Medicinal Chemistry*, https://doi.org/10.1016/j.ejmech.2020.112873.

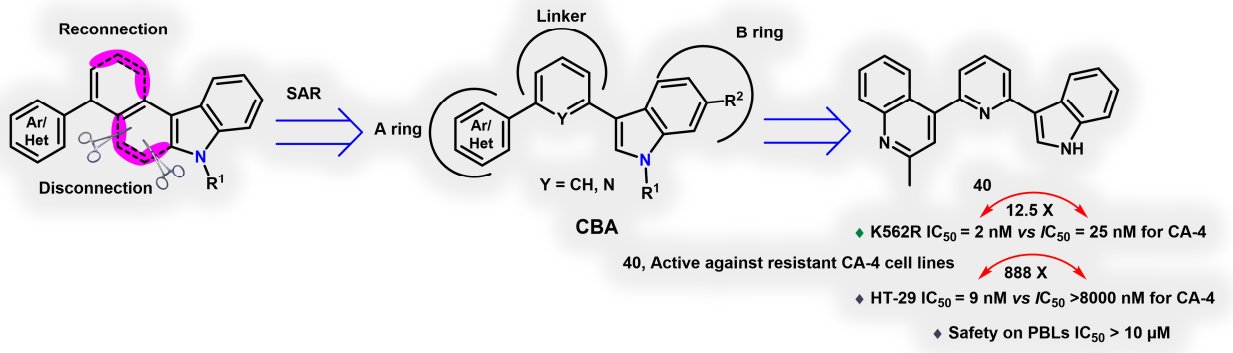

Cyclic Bridged analogs of *iso*CA-4: Design, Synthesis and Biological Evaluation

Shannon Pecnard,[a] Olivier Provot,[a,*] Hélène Levaique,[b] Jérome Bignon,[b] Laurie Askenatzis,[b] Francois Saller,[c] Delphine Borgel,[c] Sophie Michallet,[d] Marie-Catherine Laisne,[d] Laurence Lafanechère,[d] Mouad Alami,[a,*] and Abdallah Hamze[a,*]

[a] *Université Paris-Saclay, CNRS, BioCIS, 92290, Châtenay-Malabry, France.*
[b] *Institut de Chimie des Substances Naturelles, UPR 2301, CNRS, F-91198 Gif sur Yvette, France*
[c] *INSERM, UMR-S1176, University Paris-Saclay, F-94276 Le Kremlin-Bicetre, France*
[d] *Institute for Advanced Biosciences, INSERM U1209, CNRS UMR5309, Université Grenoble Alpes, Grenoble, France.*

Highlights

- Quinaldinyl-Pyridyl-Indole (QnPyInd) was discovered as novel tubulin inhibitors.
- Compound **42** displayed excellent antiproliferative activity with average IC_{50} of 5.6 nM.
- **42** exhibited high antiproliferative activity against resistant K562R and HT-29 cell lines.
- **42** inhibited tubulin polymerization both *in vitro* and in cells and induced G2/M cell cycle arrest.
- The safety profile of **42** was demonstrated in human no cancer cells PBLs.

Abstract

In this work, a series of cyclic bridged analogs of *iso*combretastatin A-4 (*iso*CA-4) with phenyl or pyridine linkers were designed and synthesized. The synthesis of the desired analogs was performed by the formation of nitro-vinyl intermediates, followed by a Cadogan cyclization. Structure activity relationship (SAR) study demonstrates the critical role of the combination of quinaldine as ring A, pyridine as the linker, and indole as ring B in the same molecule, for the cytotoxic activity. Among all tested compounds, compound **42** showed the highest antiproliferative activity against a panel of cancer cell lines with average IC_{50} values of 5.6 nM. Also, compound **42** showed high antiproliferative activity against the MDR1-overexpressing K562R cell line; thus, it was 1.5- and 12-fold more active than the reference compounds, *iso*CA-4 and CA-4, respectively. Moreover, **42** displayed a strong antiproliferative activity against the colon-carcinoma cells (HT-29), which are resistant to combretastatin A-4 and *iso*CA-4, and it was found to be 8000-fold more active than natural CA-4. Compound **42** also effectively inhibited tubulin polymerization both *in vitro* and in cells, and induced cell cycle arrest in G2/M phase. Next, we demonstrated that compound **42** dose-dependently caused caspase-induced apoptosis of K562 cells through mitochondrial dysfunction. Finally, we evaluated the effect of compound **42** in human no cancer cells compared to the reference compound. We demonstrated that **42** was 73 times less cytotoxic than *iso*CA-4 in quiescent peripheral blood lymphocytes (PBLs). In summary, these results suggest that compound **42** represents a promising tubulin inhibitor worthy of further investigation.

Keywords: tubulin inhibitor, combretastatin A-4, quinaldine, pyridine, cancer.

1. Introduction

Microtubules (MTs) are cytoskeletal filaments composed of α-and β-tubulin heterodimers, and they are essential for intracellular organization, organelle trafficking, and chromosome segregation. [1, 2] In the context of anti-cancer small-molecule drug development, dynamic microtubules continue to be among the most successful cancer chemotherapeutic targets.[3] Microtubule-binding agents (MTAs) generally interact with one of five-primary tubulin binding sites: the laulimalide, maytansine, paclitaxel/epothilone, vinca alkaloid, and the colchicine sites. They perturb mitosis and arrest cells during the G_2/M phase of the cell cycle.[4] MTAs also specifically perturb endothelial cell proliferation and migration. Thus, drugs that bind to the colchicine site undergo intensive investigation as vascular-targeting agents for cancer therapy.[5] Colchicine is not now in clinical use as an anti-cancer treatment owing to its narrow therapeutic index.[6] The combretastatins consist of a group of diaryl stilbenoid isolated by Pettit *et al.* in 1989 from the bark of the South African Bush tree *Combretum caffrum.*[7] Combretastatin-A4 (CA-4) is the prototype of this series of vascular disrupting agents (VDA).[8, 9] CA-4 has proven to be a significant cancer cell growth inhibitor and antimitotic agent through tubulin polymerization inhibition *via* binding to the colchicine binding site of tubulin. It causes rapid vascular shutdown and cell death in the tumor.[10] The water-soluble phosphate prodrug of CA-4, the CA-4P (fosbretabulin, Fig. 1), was found to inhibit tumor blood flow at concentrations 10-fold lower than its maximum tolerated dose. This observation led to the first clinical trial of CA-4 as a VDA.[11] Fosbretabulin is in phase II/III clinical trials either alone or in combination with traditional chemotherapeutic agents or radiotherapy.[12, 13] CA-4 exists as *cis*- and *trans*-stilbene isomer. Only the *cis* configuration of CA-4 possesses anti-cancer activity. Isomerization of *cis* CA-4 to less active *trans*-CA-4 is readily observed during storage, administration, and metabolism.[14, 15] SAR studies on CA-4 demonstrated that the following elements are crucial for the biological activity and the inhibition of tubulin polymerization: 1) the presence of *cis*-double bond separating the two phenyl rings; 2) the 3,4,5-trimethoxyphenyl (TMP) A-ring play an important role to maintain the activity ; 3) more modifications in terms of SAR can be done on the C3' of B-ring. Concerning the deleterious isomerization issue of natural CA-4, several heterocyclic bridging CA-4 analogs have been prepared to restrict the *cis* configuration and provide optimal bioactivity.[16] Our group has extensively reported a series of antiproliferative, tubulin-binding *iso*CA-4 compounds **3**-**5** (Fig. 1). We resolved the instability issue of CA-4, the new analogs such as *iso*CA-4, have similar inhibition of tubulin polymerization activity and cytotoxicity compared to CA-4 but show higher stability.[17-22] A few reports have attempted to modify the trimethoxyphenyl ring (ring A) with mixed outcomes. We have recently undertaken the challenge of optimizing *iso*CA-4 analogs with heterocycles, by replacing both traditional A- and B-rings. Thus, the 3,4,5-trimethoxyphenyl A ring was replaced by a quinolinyl (isoCoQuine, **6**)[23] or a quinazolinyl nuclei (isoCoQ, **7**)[24] successfully. Wang et *al.* developed a 3-atom linker containing nitrogen with a good antiproliferative activity (compounds **8** and **9**).[25] Recently, we found that classical ring B of CA-4 or *iso*CA-4 can be substituted effectively by a carbazolyl group (compound **10**).[26] Next, we noticed that the combination which associates a quinolinyl as ring A and carbazolyl group as ring B resulted in the highest potency. The Quinaldinyl-*iso*-Carbazolyl (Qn*iso*Cz) **11** compound was found more active than *iso*CA-4 against A549, U87-MG, and HUVEC cells.[27] Also, Qn*iso*Cz **11** was 67-fold more cytotoxic than CA-4 against lung adenocarcinoma epithelial cells (A549). A similar replacement as in compound **11** was also achieved with a *N*(Me) linker in compound **12**.[28]

In the continuation of our work in the study of SARs of *iso*CA-4 series and encouraged by the exciting results obtained with quinolines and quinazolines, we undertake the current study to investigate the effect of novel variation of bridge structure on the antiproliferative activities of the resulting CA-4 analogs. Precisely, we have designed, synthesized, and evaluated a series of novel cyclic bridged analogs (**CBAs**) of CA-4 having a phenyl or a pyridine linker (Fig. 1). The use of a disconnection and reconnection approach of carbazole derivatives (**10** or **11**) led us to investigate the indole nucleus as B-ring equivalent. Simultaneously, for A-ring, different combinations were studied, including the use of 3,4,5-trimethoxyphenyl (TMP), and quinolinyl groups (Fig 1). We analyzed these novel heterocyclic structures' effect on cell viability, cell cycle, and tubulin polymerization *in cells* and *in vitro*, on pure tubulin.

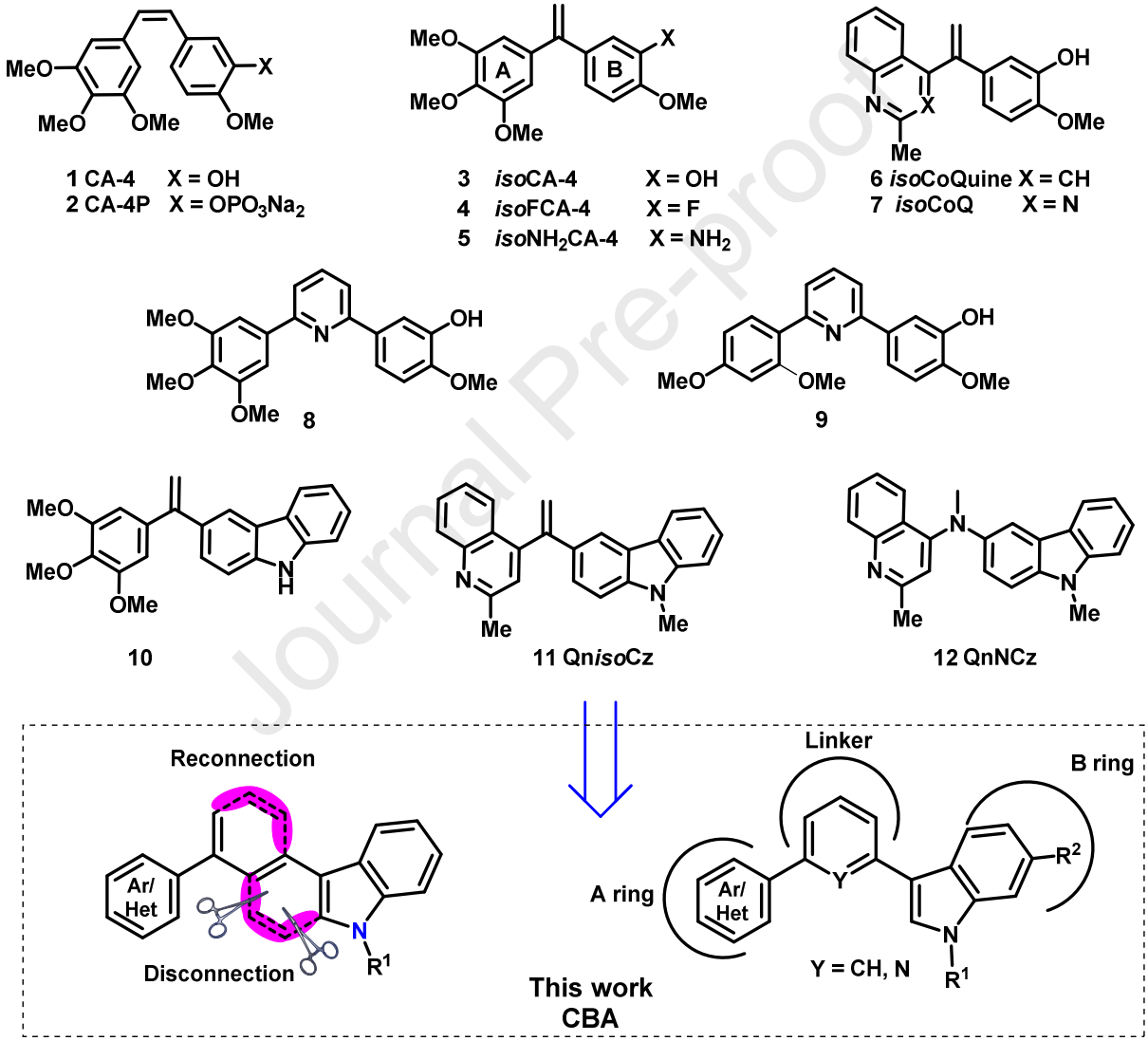

Fig. 1. Structures of CA-4, *iso*CA-4 derivatives, synthetic analogs and target **C**yclic **B**ridged **A**nalogs **CBA**

2. Results and discussion

2.1. Chemistry

First, we prepared the series of compounds having a TMP group (ring A) as in the case of CA-4 and *iso*CA-4 and a phenyl group as a linker (Scheme 1). To explore the SARs, first, modifications were realized on the indole ring. The key *N*-tosylhydrazone (NTH) derivative **15** was prepared in a two steps reaction starting from commercial 5-bromo-1,2,3-trimethoxybenzene **13** (Scheme 1). We successfully realized a Suzuki-Miyaura coupling between reagent **13** and 3-acetylphenyl-boronic acid. Then, we converted the acetophenone derivative **14** into NTH **15** in excellent yield. Next, we used our established methodology to convert this NTH to indoles.[26, 29, 30] We obtained the corresponding derivatives **16**-**19** in a moderate yield after two steps: the first consists of the formation of 1-nitro-2-(1-phenylvinyl)benzene intermediates by coupling **15** and the appropriate 1-bromo-2-nitrobenzene derivative, whereas, in the second step, all the generated intermediates were the subject to Cadogan cyclization without prior purification.[31] To explore the importance of free NH-indole on the biological activity, we also realized the *N*-methylation of compound **16**. We obtained the *N*-methylated indole **20** in a moderate yield (53%).

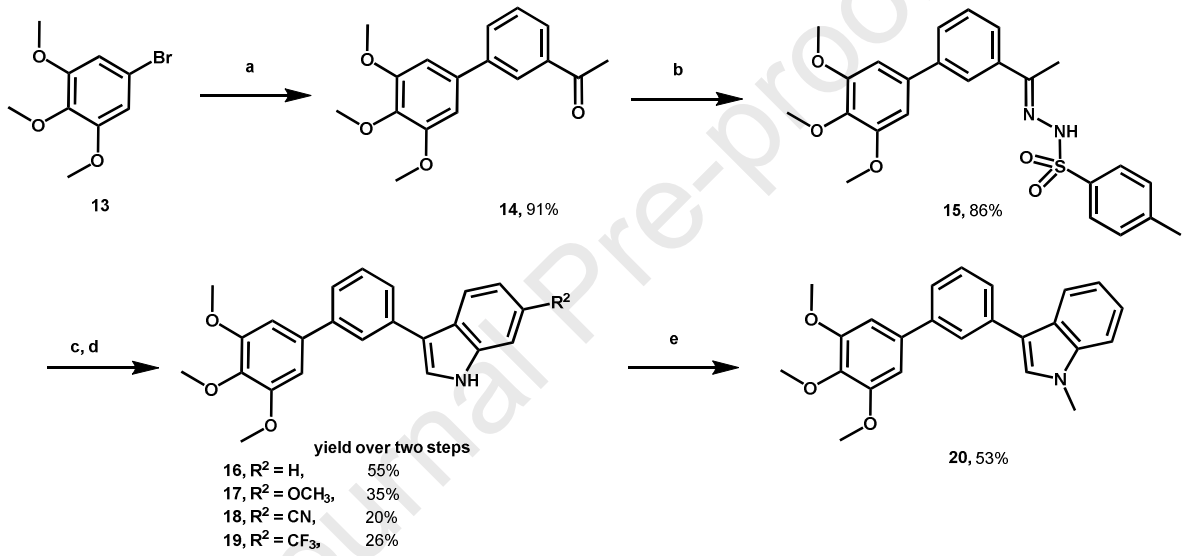

Scheme 1. Reagents and conditions: (a) 3-acetylphenyl-boronic acid, $Pd(OAc)_2$, SPhos, $K_3PO_4.H_2O$, cyclopentyl methyl ether (CPME)/H_2O, 110 °C; (b) 4-methylbenzenesulfonohydrazide, EtOH, reflux; (c) Appropriate 1-bromo-2-nitrobenzene derivative, $Pd_2dba_3.CHCl_3$ (5 mol%), XPhos (10 mol%), LiO*t*Bu, dry dioxane, 110 °C overnight, after filtration on Celite and evaporation, compounds were subject to Codagan cyclization; (d) $MoO_2Cl_2(dmf)_2$ (10 mol %), PPh_3 (4 equiv), in 3 mL of dioxane under microwave irradiation (MWI) at 135 °C; (e) NaH, CH_3I, DMF, rt.

As in our previous SAR studies, we demonstrated the possibility of the change of TMP part by a heterocyclic ring with similar or better activity. Next, we replaced the TMP ring present in compounds **16**-**20** by a quinoline nucleus to prepare a second series of *bis*-heterocyclic derivatives **28**-**31** (Scheme 2). First, the starting material **22** was prepared by a Negishi coupling starting from 2,4-dichloroquinoline **21** and $Zn(CN)_2$ under Pd-catalysis in excellent yield. We prepared acetophenone derivatives **24**-**25** by a Suzuki-Miyaura coupling between **22** or commercial 4-chloro-2-methylquinoline **23** and 3-acetylphenyl-boronic acid. The conversion of these acetophenones to NTH **26**-**27** was realized easily by treatment with 4-methylbenzenesulfonohydrazide in refluxing EtOH. Again, we used our methodology[26, 29, 30, 32-34] to convert the NTH **26**-**27** to indoles in two steps, and the corresponding desired compounds **28**-**29** were obtained in moderate to good yield. To study the importance of free indole in the series, on the biological activity, we masked this amine either by

a methyl or hydroxymethyl group, starting from compound **29**. We obtained compound **30** in a good yield, by simple *N*-methylation. While compound **31** was obtained in a moderate yield after formylation and treatment in a basic media.

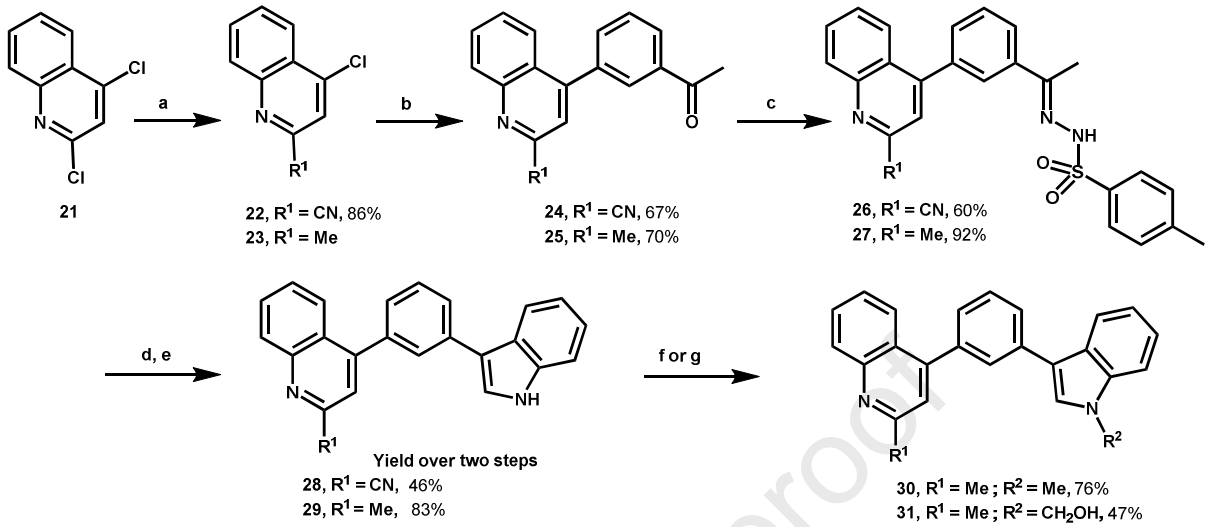

Scheme 2. (a) $Pd(PPh_3)_4$, $Zn(CN)_2$, DMF, 120 °C; (b) 3-acetylphenyl)boronic acid, $Pd(PPh_3)_4$, $K_3PO_4.H_2O$, Dioxane/H_2O, 110 °C; (c) 4-methylbenzenesulfonohydrazide, EtOH, 95 °C; (d) 1-bromo-2-nitrobenzene $Pd_2dba_3.CHCl_3$ (5 mol%), XPhos (10 mol%), LiO*t*Bu, dry dioxane, 110 °C overnight, after filtration on Celite and evaporation, the crude was subject to Codagan cyclization; (e) $MoO_2Cl_2(dmf)_2$ (10 mol %), PPh_3 (4 equiv),), in 3 mL of dioxane under MWI at 135 °C; (f): NaH, CH_3I, DMF, rt; (g): $NaOH_{aq}$, $HCOH_{aq}$, EtOH, rt.

As Wang *et al.* demonstrated the utility of the use of a pyridine bridge as a linker on the SAR study of CA-4 analogs,[25] we, next, changed the linker between the A- and B-rings, from phenyl to pyridine nucleus (Scheme 3). We followed the same strategy depicted in Scheme 1 and 2. We obtained compounds **35-37** in moderate to good yield (Scheme 3). For the synthesis of compound **42**, we first realized the synthesis of bromopyrdine derivative **40**, and then, we performed the Suzuki-Miyaura coupling with 2-methylquinolin-4-yl)boronic acid. The indole formation was realized by Cadogan cyclization to give compound **42** in a 75% yield. Finally, *N*-methylation of the indole nucleus of **42** led to compound **43** in excellent yield.

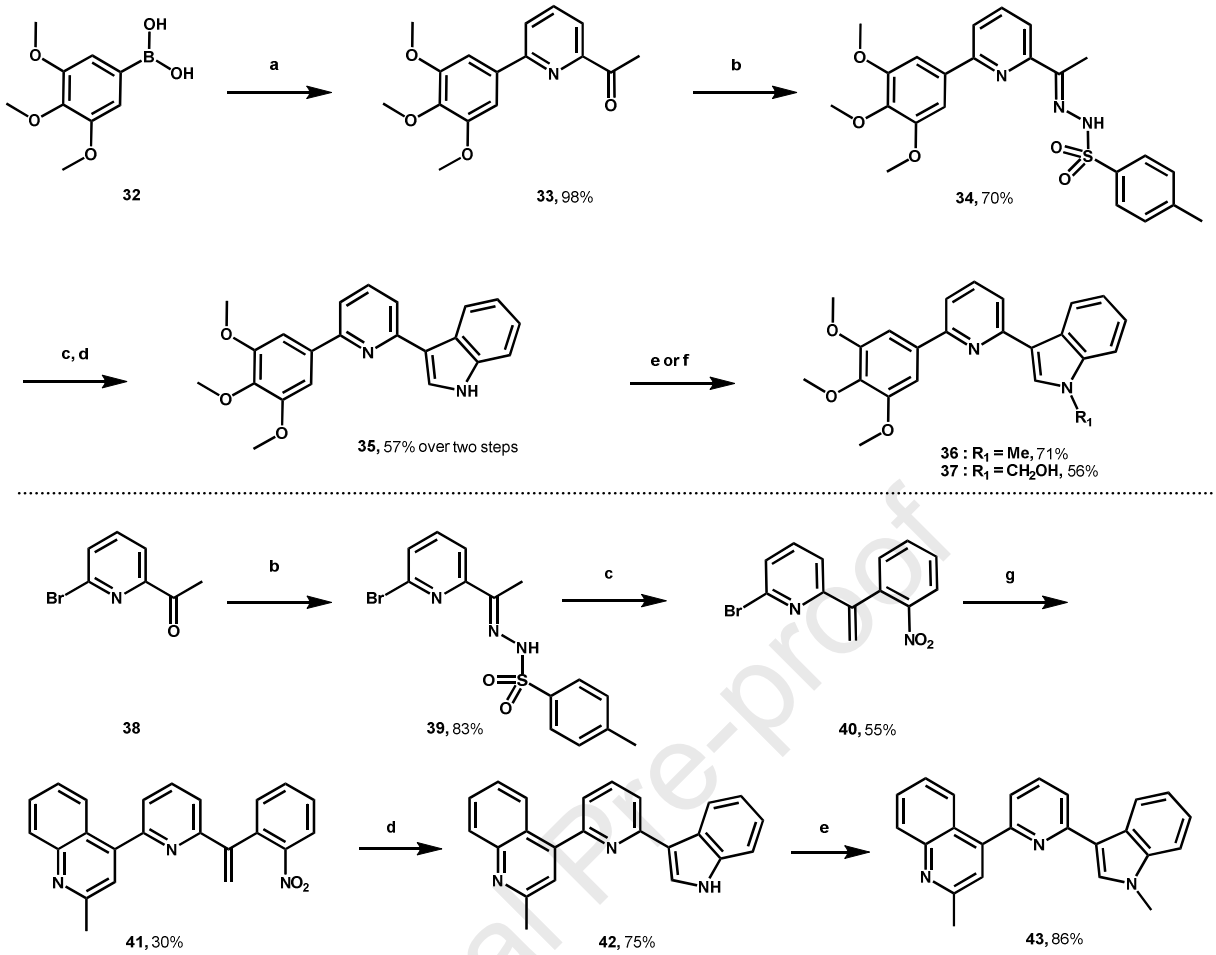

Scheme 3. (a) 3,4,5-trimethoxyphenylboronic acid, 1-(6-bromopyridin-2-yl)ethanone, $Pd(OAc)_2$, PPh_3, K_2CO_3, dioxane/H_2O, 110 °C, overnight; (b) (4-methylbenzenesulfonohydrazide, EtOH, 95 °C; (c) 1-iodo-2-nitrobenzene, $Pd_2dba_3.CHCl_3$ (5 mol%), XPhos (10 mol%), Li*O*t*Bu*, dry dioxane, 100 °C overnight; (d) $MoO_2Cl_2(dmf)_2$ (10 mol %), PPh_3 (4 equiv), in 3 mL of dioxane under MWI at 135 °C; (e) NaH, CH_3I, DMF, rt; (f) (33), $NaOH_{aq}$, $HCOH_{aq}$, EtOH, rt; (g) 2-methylquinolin-4-yl)boronic acid, $Pd_2dba_3.CHCl_3$, SPhos, K_2CO_3, 100 °C.

Finally, to obtain the two reference compounds necessary for SAR study, compounds **47[35]** and **8[25]** were prepared in an acceptable yield, by a two sequential Suzuki-Miyaura cross-coupling (Scheme 4) starting from (3-bromophenyl)boronic acid (**44**) and 2,6-dibromopyridine (**48**) respectively.

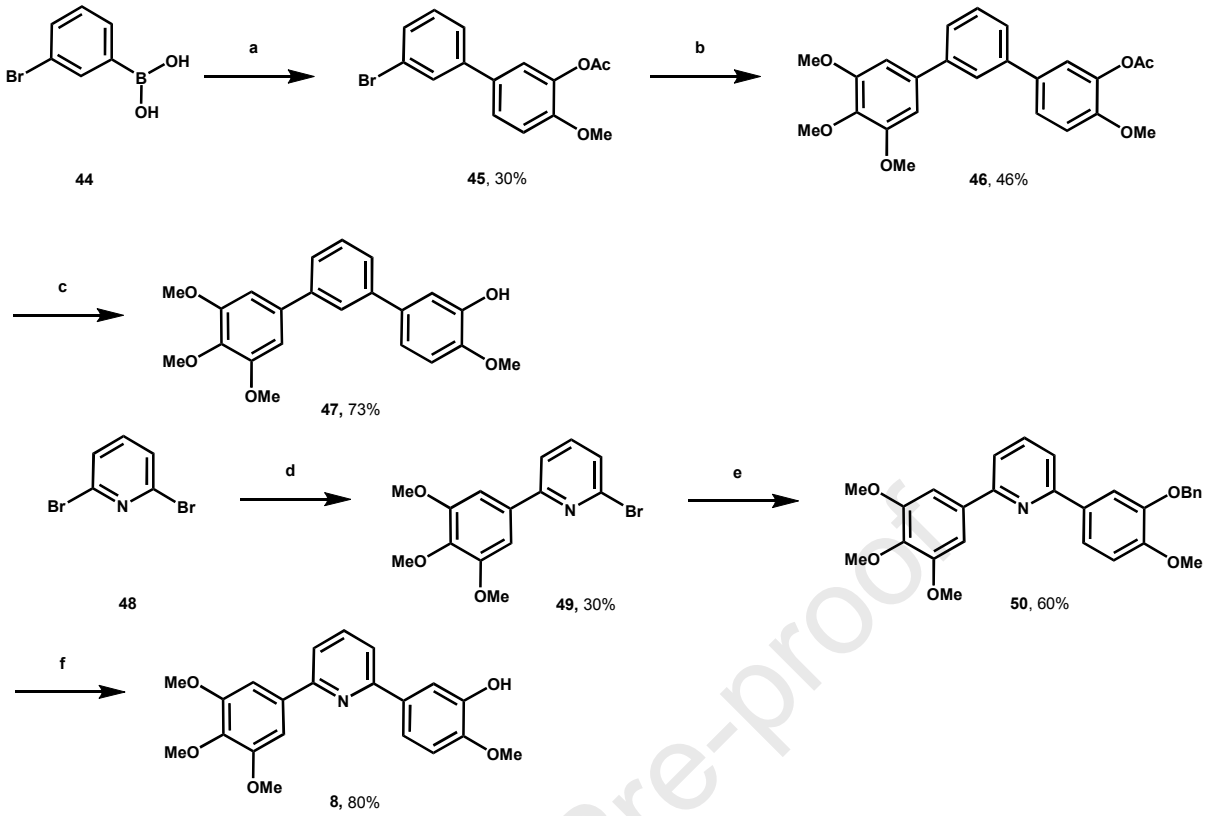

Scheme 4. (a) 5-iodo-2-methoxyphenyl acetate, $Pd(PPh_3)_4$ (2 mol%), K_2CO_3,Toluene/H_2O (4:1), 110 °C, 1 h; (b) (3,4,5-trimethoxyphenyl)boronic acid, $Pd(PPh_3)_4$ (2 mol%), K_2CO_3, Toluene/H_2O (4:1), 110 °C, 1 h; (c) K_2CO_3 (10 eq), MeOH, 50 °C, overnight; (d) (3,4,5-trimethoxyphenyl)boronic acid, $Pd(OAc)_2$ (5 mol%), $P(Cy_3).BF_4$ (10 mol%), K_2CO_3, Toluene/H_2O (30:1), 110 °C, 20 min; (e) (3-(benzyloxy)-4-methoxyphenyl)boronic acid, $Pd(OAc)_2$ (5 mol%), PPh_3 (10 mol%), K_2CO_3, Dioxane/H_2O (2:1), 110 °C, 1 h; (f) Pd/C H_2, (10 mol%), EtOH, rt, overnight.

2.2. Biological effects of the new compounds

2.2.1. Effects on cell viability

In a first approach, the effect of the new compounds on cell viability was evaluated on a human colon cancer cell line (HCT116), as mentioned in Table 1, in parallel with *iso*CA-4 and CA-4 as experimental controls. We determined their effect on cell viability by using the sensitive CellTiter-Glo® luminescent assay, a homogeneous-method to determine the number of viable cells in culture and based on the quantitation of the ATP (an indicator of metabolically active cells). The amount of ATP is directly proportional to the number of viable cells present in the culture.

As shown in Table 1, in the series of the compounds having a phenyl ring as a linker, compound **16** having the TMP ring demonstrates significant antiproliferative activity with an IC_{50} of 70 nM. When a substituent such as methoxy (compound **17)**, nitrile (compound **18)**, or trifluoromethyl group (compound **19)**, was introduced on position C6 of indole nucleus, the cytotoxicity is no longer observed, suggesting that such a substitution of the indole ring does not favor binding of the compound to the colchicine site or impairs the ability of the compounds to penetrate the cells. When the NH of indole was methylated (compound **20**), a less cytotoxic activity (drop by a factor 7) was obtained compared to compound **16**, which has a free indole ring. Next, based on our previous SARs,

we carried out the replacement of the TMP nucleus by a quinoline having a substituent in position C2 (compounds **28**-**31**). 2-Quinolinecarbonitrile nucleus **28** displayed a modest antiproliferative activity (less active than **16**). To our surprise, however, compound **29** having a quinaldine as A-ring showed about 2-fold higher activity in comparison to **16**. Again, modifications of the indole ring reduce the cytotoxic activity as the *N*-methylated indole **30** or (indol-1-yl)methanol **31** derivatives were less potent than compound **29** having the free NH-indole. To better understand the influence of the nature of A- and B-rings on the cytotoxicity activity, in this series containing a phenyl ring as the linker, we compared reference compound **47**[35] having the same TMP (ring A) and 2-methoxyphenol (ring B) as in the structure of CA-4 and *iso*CA-4. This compound showed low antiproliferative activity (around 60- and 114-fold less active then **16** and **29** respectively), suggesting that the quinaldine and indole nucleus interact better with the colchicine-binding site. Wang *et al.* have demonstrated that the use of a pyridine bridge between the TMP ring A and 2-methoxyphenol B of CA-4 induces an interesting antiproliferative activity.[25] Therefore, we included in our SAR study the analysis of the effect of such pyridine linker. As shown in Table 1, this replacement led to a significant increase of the cytotoxicity activity in comparison with the phenyl linker: compound **35** having the TMP ring exhibited an IC_{50} of 20 nM (3.5-fold higher than **16**), and even better, compound **42** having quinaldine ring showed high antiproliferative activity with low single-digit nM (IC_{50} value 2.2 nM, 18-fold more active than **29**) in the HCT116 cell line. The activity obtained with **42** is comparable to those of prior lead *iso*CA-4 and CA-4 in the same assays, thus indicating that the A/B-ring system is changeable and favorable bioisosteres include quinaldine and indole moieties. Again, we synthesized and tested compound **8**, having pyridine linker and ring A and B as the natural CA-4. We found that this compound had low cytotoxicity against HCT-116 cells; this demonstrates the critical role played by the combination of quinaldine as ring A, pyridine as the linker, and indole as ring B in the same molecule, for the cytotoxic activity (Fig. 2).

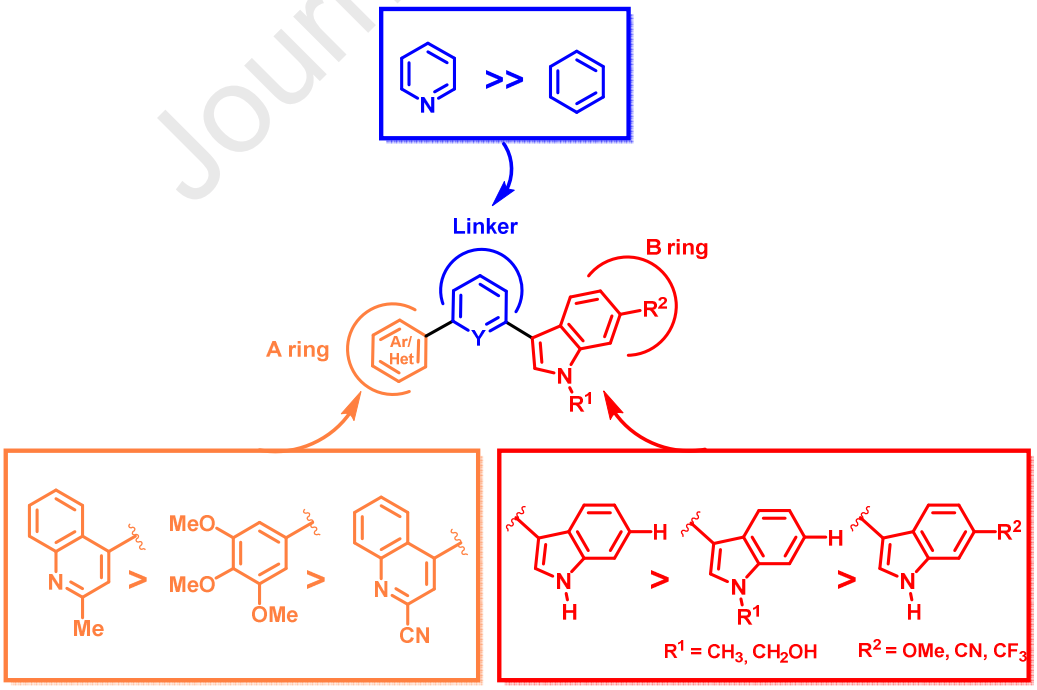

Fig. 2. Summary of the SARs study of target compounds based on cell viability evaluated on a human colon cancer cell line.

compd		HCT116 (nM)[b]	compd		HCT116 (nM)[b]
16	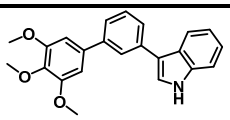	70 ± 15	**35**	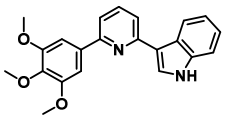	20 ± 1.9
17	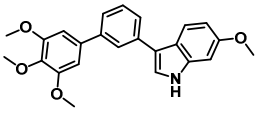	4910 ± 600	**36**	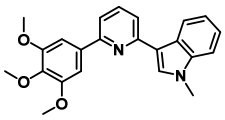	400 ± 150
18	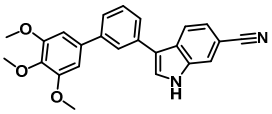	7630 ± 650	**37**	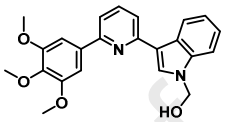	90.2 ± 1.7
19	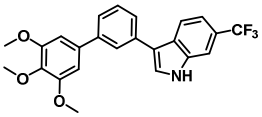	3220 ± 780	**42**	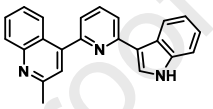	2.2 ± 0.4
20	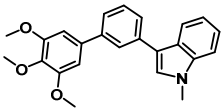	490 ± 120	**43**	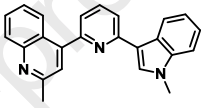	267 ± 26
28	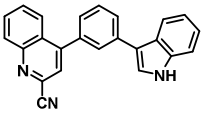	175 ± 21.2	**47**	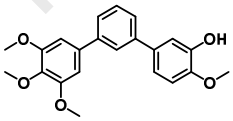	4564 ± 148
29	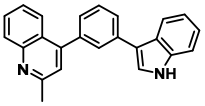	40 ± 1.4	**8**	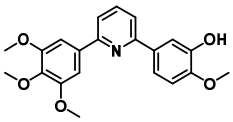	1300 ± 120
30	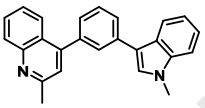	70 ± 4.2	**1** CA-4	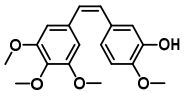	2.6 ± 0.6[c]
31	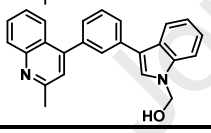	79 ± 19	**3** *iso*CA4	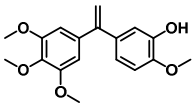	2.4 ± 0.9

Table 1. Effect of designed compounds on HCT116 cell viability.[a]

[a] HCT-116 human colon carcinoma cells. [b] Compound concentration required to decrease cell growth by 50%; values represent the average SD of three experiments. [c] The IC_{50} value for CA-4[36] and *iso*CA-4[37, 38] were determined in this study.

After this first screening on HCT116 viability, the most active compound Quinaldinyl-Pyridyl-Indole (**QnPyInd**) **42** was selected for evaluation against six additional human cancer cell lines and compared with the reference compound *iso*CA-4 (Table 2). QnPyInd **42** displayed a nanomolar level of cytotoxicity against HCT116, K562, K562R, MiaPaca, A546, MCF7 and HT29 cancer cells with an IC_{50} ranging from 2.2 to 10 nM. With average IC_{50} values of 5.6 nM, compound **42** appeared to be more active than the reference compounds (*iso*CA-4 and CA-4, the average of IC_{50} values were 78 and > 1000 nM, respectively). To further explore this new molecule's potential, we measured the cytotoxic effect of our lead compounds **42** on multidrug-resistant (MDR) leukemia cells. Parental K562 cells and MDR1-overexpressing K562R cells were employed and compared in this study. The biological evaluation revealed that **42** showed high antiproliferative activity against the K562R cell line, with an IC_{50} of 2.4 nM; thus, it was 1.5- and 12-fold more active than the reference compounds, *iso*CA-4 and

CA-4, respectively. The antiproliferative activity of **42** is as important in the MDR1 overexpressing K562R cell line as in the parental K562 cell line, indicating that this lead compound is not a substrate for P-glycoprotein (Pgp). Cytotoxic activities of compound **42** and *iso*CA-4 were equipotent against lung and breast cancer cells (A549 and MCF7). However, QnPyInd **42** was 25- and 17-fold more active than CA-4 against A549 and MCF7 cell lines, respectively. Next, we evaluated compound **42** on the colon-carcinoma cells HT-29, which are resistant to combretastatin A-4 because of the overexpression of a multidrug-resistance protein (MRP-1).[39] As depicted in Table 2, compound **42** displayed an intense antiproliferative activity against this resistant cell line, with a nanomolar IC_{50} value of 9.1 nM, confirming that **42** is not a substrate of efflux pumps. The two reference compounds *iso*CA-4 and especially CA-4 were found inactive against HT-29 resistant cells, with IC_{50} values of 275 and > 8000 nM, respectively. The differential activity of CA4, *iso*CA4, and compound **42** can be explained by the structural resemblance between *iso*-CA-4 and CA-4, which can be a substrate of MRP-1. In contrast, the new structure of **42** allows it to escape the detoxifying actions of these proteins overexpressed in HT-29 cells. Also, *iso*CA-4 and CA-4 share a meta-hydroxy group on the B-ring, which is partially mediated by the MRP-1 transporter and can favorably eliminate glucuronidated phenols.[40] Compound **42**, lacking the *meta*-OH group in the B-ring, was highly active in HT-29 cells.

Analyzing the physicochemical properties of compound **42** in comparison to the two references compounds CA4 and *iso*CA-4 shows that **42** is more lipophilic, with clogP of 5.2, compared to clogP of 3.3 for CA-4 and 3.15 for *iso*CA-4. Furthermore, in view of the powerful antiproliferative activity of **42** (Table 2), this compound could find application for the treatment of glioblastoma because of its potential ability to cross the blood–brain barrier.

Table 2. Effects on cell viability of compound **42** against a panel of seven human cancer cell lines, IC_{50} values are reported in nM.

Compd	**HCT116**[a]	**K562**[b]	**K562R**[c]	**MiaPaca2**[d]	**A549**[e]	**MCF7**[f]	**HT-29**[h]
Tumor Type	Colon	Leukemia	Leukemia	Pancreas	Lung	Breast	Colon
42	2.2 ± 0.4	4.5 ± 0.5	2.0 ± 0.9	3.6 ± 0.4	8.0 ± 0.25	10.1 ± 1.0	9.1 ± 0.38
***iso*CA4**	2.4 ± 0.9	5.2 ± 0.2	3.0 ± 0.2	10 ± 1.2	10 ± 0.1	8 ± 0.4	275 ± 22
CA-4	2.7 ± 0.3	5.5 ± 0.4	25 ± 0.05	8 ± 2	200 ± 5	170 ± 5	>8000

[a] Colon-carcinoma cells (HCT116); [b] Chronic myelogenous leukemia cells (K562); [c] Doxorubicin-resistant chronic myeloid leukemia cells (K562R); [d] Human pancreatic carcinoma (MiaPaca2); [e] Adenocarcinoma human alveolar basal epithelial cells (A549); [f] Breast cancer cell line (MCF-7); Human colon cancer cell line (HT-29).

2.2.2. Effect on Cell Cycle.

The cytotoxicity test probes all vital cell functions. To get further insights into the mechanism of action of the new active compound, we investigate the effect of **42** on cell cycle progression. Thus, we conducted a flow cytometry analysis and analyzed the effect of a 24 hour-treatment with different concentrations (20, 50, 100 nM) of compound **42** on the fate of K562 cells. As shown in Fig. 3, when we treated cells with compound **42**, the number of cells in G_2/M increases in a dose-dependent manner. A large part of the cells (81 %) is blocked in G2/M when **42** is at a 100nM concentration. These results indicate that this compound induced a cell cycle arrest in mitosis.[17, 18], suggesting that this new compound targets tubulin.

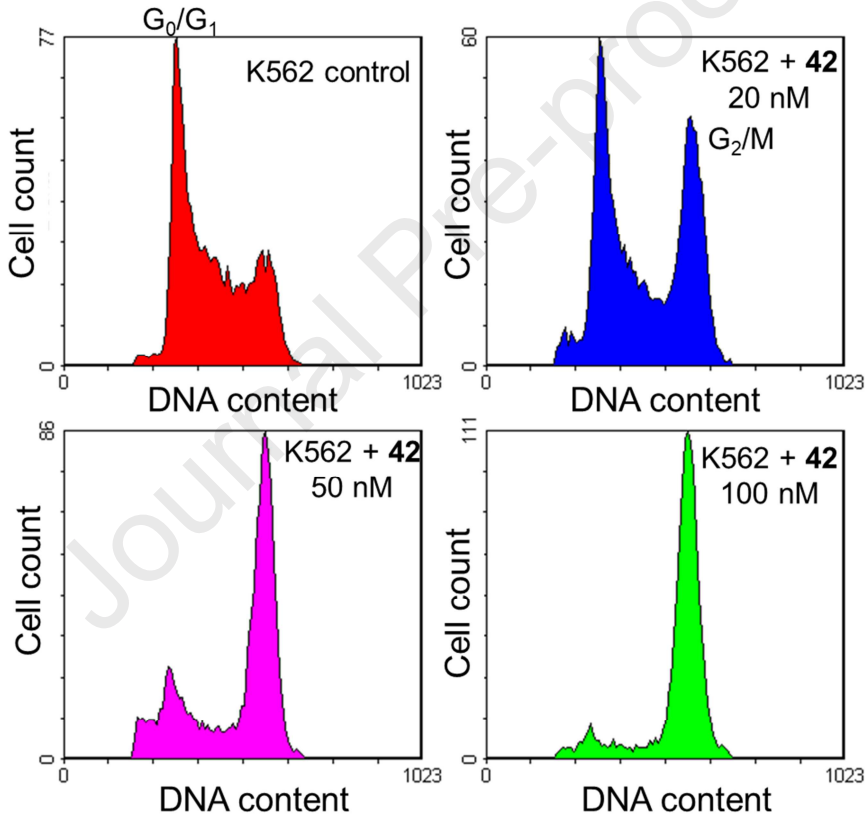

	G0/G1	S	G2/M
NT	22,8	60,2	17
20 nM	23,4	40,9	35,7
50 nM	19,8	22,6	57,6
100 nM	5,6	13,1	81,3

Fig. 3. Effect of compound **42** on the cell cycle of K562 cell lines. One representative replicate out of two is shown.

2.2.3. Effect on cell microtubule network.

To analyze the effect of the compound on cell microtubules, we used a variant of a recently described sensitive cell-based assay,[41] which quantifies the amount of microtubules present in cells. We compared the depolymerizing effect of **42** to CA-4 and *iso*-CA4. As shown in Fig. 4, after 2 h of incubation, we observed that **42** was indeed able to induce dose-dependent depolymerization of the microtubule network, with complete depolymerization observed for a 5 µM concentration. In the assay, compound **42 (**IC_{50} = 0.4 µM), was found less potent than CA-4 and *iso*-CA4 (IC_{50} of 7 nM and 8 nM, respectively).

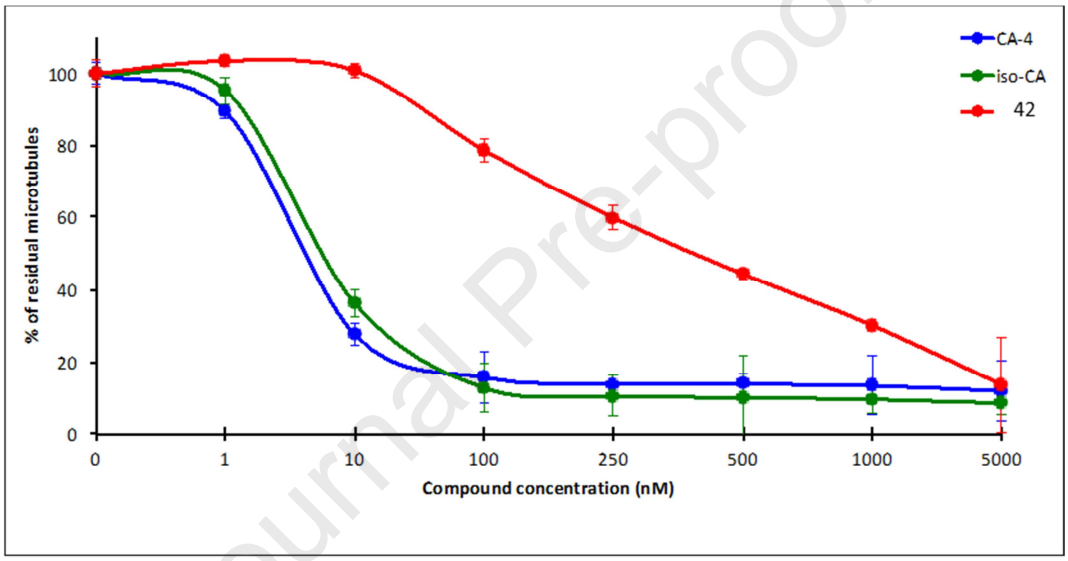

Fig. 4. Comparative analysis of the effect of **42**, CA-4, and *iso*-CA4 on microtubule dynamics in HeLa cells**.** Different doses of the compounds were applied to HeLa cells in microplates and the amount of residual microtubules was assessed after 2 hours, using a luminescent assay described in the material and methods section. Results are expressed as mean ± SEM of their independent experiments.

2.2.4. Effect on *in vitro* tubulin polymerization

The effect of compound **42** on *in vitro* tubulin polymerization (Fig. 5A) was compared to the effect of CA-4 (Fig. 5B) by monitoring absorbance at 350 nm. Indeed, light is scattered by microtubules to the extent that it is proportional to the microtubule polymer concentration.[42] Tubulin (50 µM) was pre-incubated for 30 min with different concentrations of **42** or CA-4 at 4 °C. The formation of microtubules was induced by raising the temperature to 37 °C and adding GTP (1 mM).
As shown in Fig. 5A, compound **42** inhibited pure tubulin polymerization in a dose-dependent manner, showing that it can bind tubulin directly. In these experimental conditions, the estimated concentration to inhibit 50% of the polymerization was found twice fold higher for **42** (5 µM) than for CA-4 (2.5 µM). Thus, although **42** can bind tubulin, it is a little less active than CA-4**.**

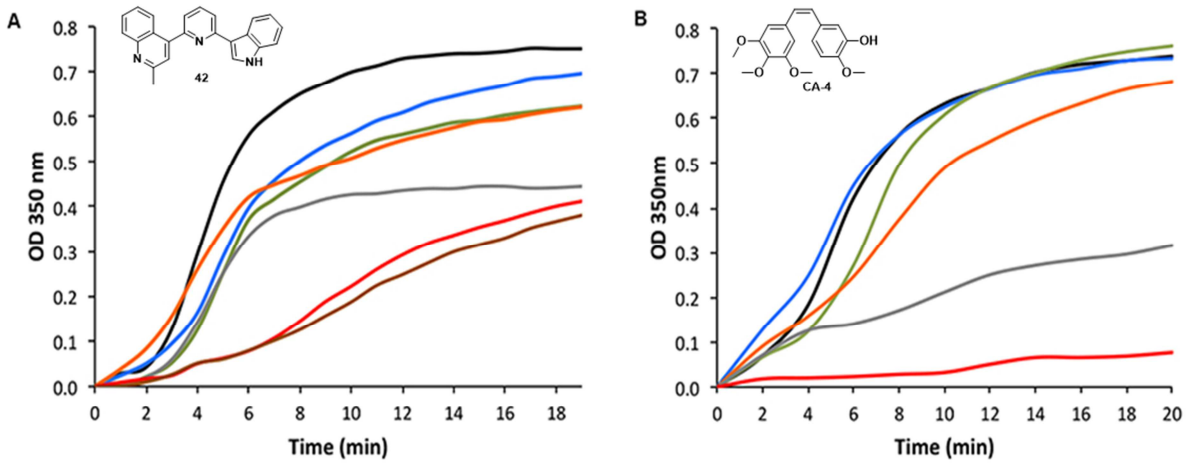

Fig. 5 Comparison of the effect of compound **42** and CA-4 on tubulin polymerization. Compound **42** (A) or CA-4 (B) were added at different concentrations to 50 µM tubulin and their effect on tubulin kinetics assembly was monitored. Black: DMSO (control); blue: 0.1 µM; green: 0.5 µM; orange: 1 µM; grey: 2.5 µM; red: 5 µM; brown: 7 µM. Representative curves of two independent experiments.

2.2.5. Effects of compound 42 on Mitochondrial Dysfunction in K562 Cells

Mitochondria play critical roles in cellular metabolism, homeostasis, and stress responses by generating ATP for energy and regulating cell death.[43] Mitochondrial dysfunctions is usually caused by depolarization and is the early hallmark of toxicity mediated through caspase-induced apoptosis.[44] As shown in Fig. 6, compound **42**-induced mitochondrial dysfunction was detected using a fluorescence-based mitochondria-specific voltage-dependent dye, JC-1. Thus, our results showed that **42** induced mitochondrial dysfunctions in a concentration-dependent manner, with significant effects beginning at a concentration of 20 nM. Our study provides convincing evidence indicating that compound **42** dose-dependently caused caspase-induced apoptosis of K562 cells through mitochondrial dysfunction.

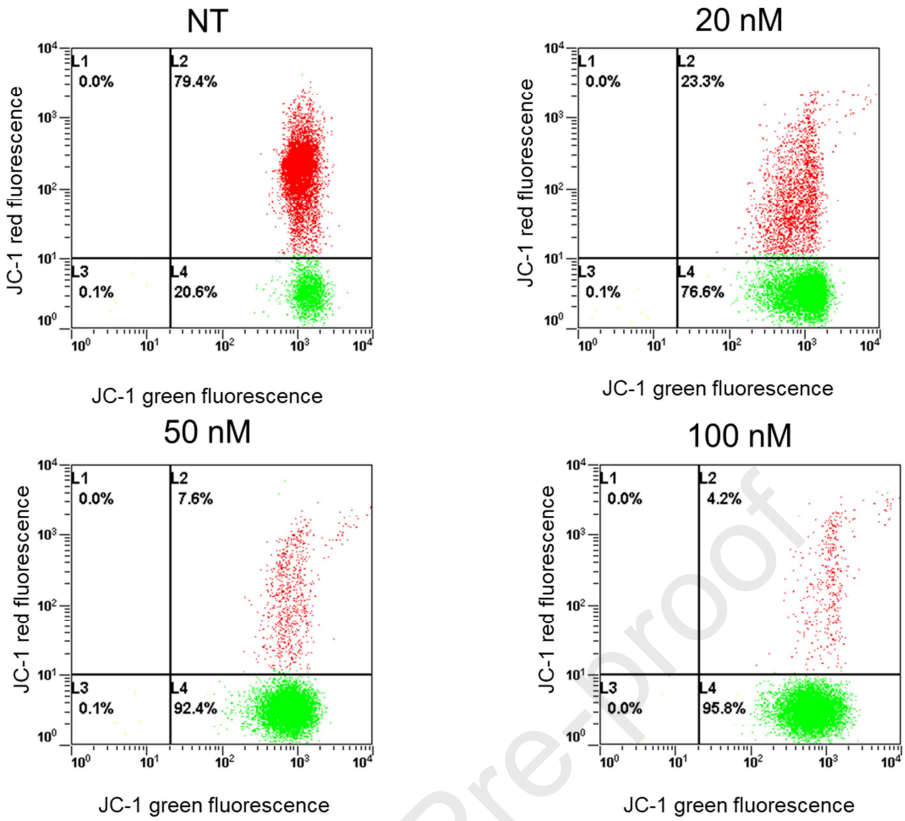

Fig. 6 Compound **42** induced mitochondrial dysfunctions in K562 leukemia cells. Cells were incubated with **42** at concentrations of 20, 50, 100 nM for 24 h at 37 °C. The portion of mitochondria dysfunction was measured using the JC1 assay.

2.2.6. Effect of compound 42 and the reference compound *iso*CA-4 in peripheral blood lymphocytes (PBLs).

To evaluate the safety profile and the cytotoxic potential of compound **42** in human no cancer cells, we compared its cytotoxicity to that of the reference compound *iso*CA-4 in quiescent peripheral blood lymphocytes (PBLs) isolated from one healthy donor. Under our experimental conditions, dose-response curves (Fig. 7A) yielded IC_{50} values of 137 nM and >10 µM for *iso*CA-4 and compound **42**, respectively. This clearly indicated that compound **42** was far less cytotoxic than *iso*CA-4 in quiescent PBLs, with a difference of at least two orders of magnitude. The proliferation of PBLs from the same donor was also induced by the potent mitogen PHA, and in agreement with previous results,[45] *iso*CA-4 was more cytotoxic in proliferating than in quiescent PBLs. However, as in quiescent PBLs, compound **42** was again less cytotoxic than *iso*CA-4 (IC_{50} value of 114 nM and 4.3 nM for compound **42** and *iso*CA-4, respectively) (Fig. 7B). Together, these results very interestingly supported a better safety profile for compound **42** than for *iso*CA-4.

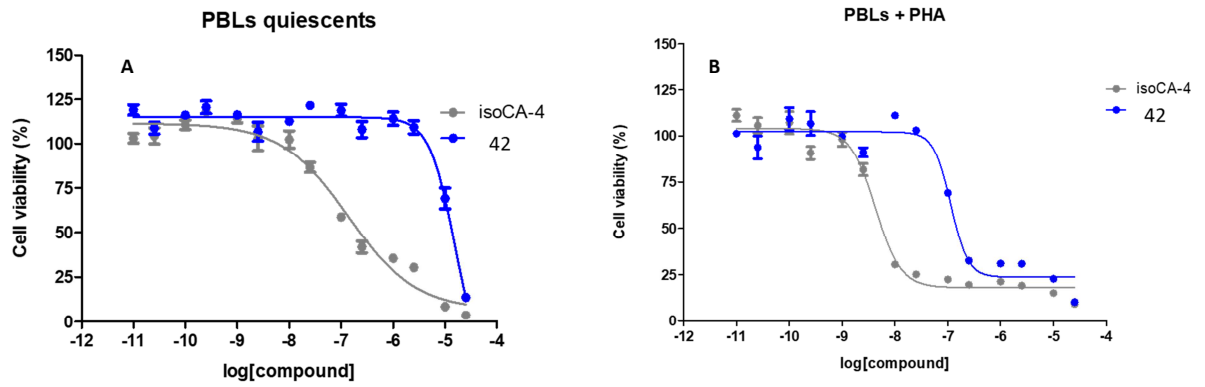

Fig. 7. Cytotoxicity of compound **42** and *iso*CA-4 in peripheral blood lymphocytes (PBLs). (A) Quiescent PBLs (10.000/well) from one healthy donor were treated in triplicate with various concentrations (10-11-2.5 x 10^{-5} M) of *iso*CA-4 and compound **42** for 72 h at 37 °C, and cell viability was measured by a luminescent assay. A cell viability of 100% corresponds to the mean luminescence value obtained for vehicle (0.25% DMSO)-treated PBLs, and data represent the mean (± standard error of the mean, SEM). Dose-response curves were fitted to a log(inhibitor) *vs* response curve using the Graph Pad Prism software, yielding IC_{50} values of 137 nM and >10 µM for *iso*CA-4 and compound **42**, respectively. Compounds could not be tested at higher concentrations than 25 µM, precluding more accurate determination of the IC_{50} value for compound **42**. (B) PBLs from the same donor (10.000/well) were activated with phytohemagglutinin (PHA. 2.5 µg/mL) to induce their proliferation, and were subsequently treated in triplicate with various concentrations (10-11-2.5 x 10^{-5} M) of *iso*CA-4 and compound **42** for 72 h at 37 °C. Cell viability was calculated as described for quiescent PBLs, and data represent the mean (± standard error of the mean, SEM). Dose-response curves were fitted to a log(inhibitor) vs response curve using the Graph Pad Prism software, yielding IC_{50} values of 4.3 nM and 114 nM for *iso*CA-4 and compound **42**, respectively.

2.3. Docking study

We performed molecular docking for compound **42** within the colchicine binding site of tubulin β subunit (the structure obtained from the X-ray crystal structure with accession code 6H9B).[27] The overall binding mode observed matched that previously known for *iso*CA-4 as well as with compound **10**, with the quinaldine ring system being accommodated by the lipophilic pocket ordinarily occupied by the trimethoxyphenyl nucleus of *iso*CA4, as well as the indole ring sitting at the same place as the B ring of *iso*CA-4. Interactions that can be expected given this binding mode hypothesis include notably (see Fig. 8) a potential hydrogen bond between the side-chain SH group of the cysteine β241 residue and the endocyclic nitrogen atom of the quinaldine moiety. The contribution of this interaction to the overall binding is reinforced by the contact between the northern part of the pyridine linker and the hydrophobic part of the side chain of lysine β254 as well as the indole moiety being sandwiched between hydrophobic parts of the side chains of lysine β352 and that of asparagine β258.

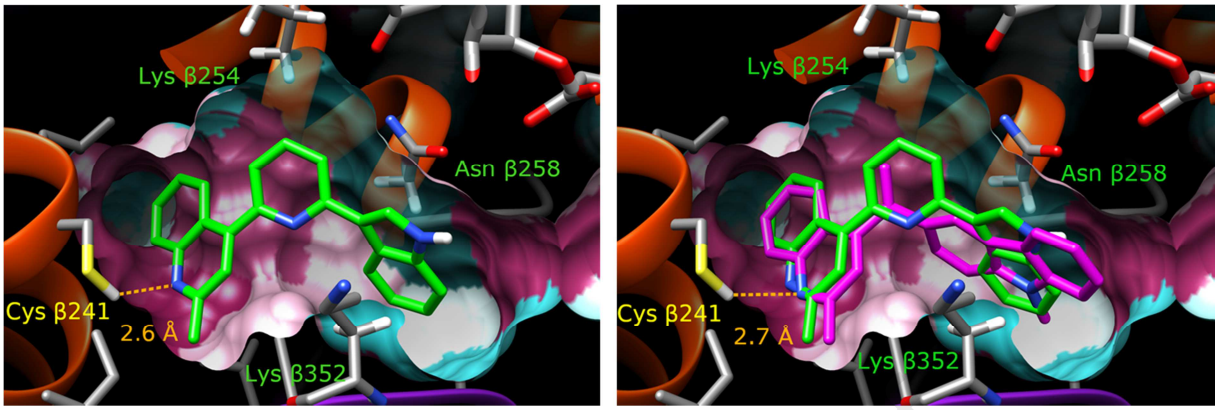

Fig. 8. (a) Putative binding mode of compound **42** (green color) within colchicine binding site of tubulin X-ray structure (accession code 6H9B). (b) same figure with previously reported binding mode of reference compound **11** in overlay (magenta color). Showing expected hydrogen bonds between nitrogen of quinoline moiety and cysteine β241, and plausible hydrophobic interactions.

3. Conclusion

In this work, we have designed and synthesized a series of Cyclic Bridged Analogs CBA derivatives of *iso*combretastatin A-4 with different aryl or heteroaryl cycles as A- ring and indole as B ring. After the SAR study, we found that the best combinations associate in their structures *(i)* quinaldine nucleus as an A ring *(ii)* connected to the pyridine as a linker and *(iii)* an indole nucleus as B-ring. The more interesting compound in these novel series is Quinaldinyl-Pyridyl-Indole (QnPyInd) **42**, which displayed a promising antiproliferative activity against seven human cancer cell lines. Besides, the new tri heterocyclic derivative **42** demonstrated high cytotoxic activity in PGP overexpressing multidrug-resistant leukemia cells (K562-R) and highly multidrug- and CA-4-resistant HT-29 cells; this result is of considerable significance given that the expression of Pgp is frequently associated with clinical resistance to chemotherapy. Compound **42** directly targets tubulin, as indicated by its ability to inhibit pure tubulin polymerization *in vitro*. Interestingly, although its depolymerizing microtubules activity is less important than CA-4 and *iso*CA, both *in vitro* and in cells, compound **42** has a cytotoxic activity at least as high as that of CA-4 and *iso*CA. Although we cannot formally exclude that **42** has other targets than tubulin, our results support the conclusion that this small microtubule depolymerizing activity is sufficient to trigger cell cycle arrest and apoptosis. Finally, we demonstrated the cytotoxic potential of compound **42** in human no cancer cells compared to the reference compound, and it was far less cytotoxic than *iso*CA-4 in quiescent PBLs.

4. Experimental

4.1. General considerations

Solvents and reagents are obtained from commercial suppliers and were used without further purification. Analytical TLC was performed using Merck silica gel F254 (230-400 mesh) plates and analyzed by UV light or by staining upon heating with vanillin solution. For silica gel chromatography, the flash chromatography technique was used, with Merck silica gel 60 (230-400 mesh) and p.a. grade solvents unless otherwise noted. The ^{1}H NMR and ^{13}C NMR spectra were recorded in either $CDCl_3$, MeOD, or DMSO-d_6 on Bruker Avance 300 or 400

spectrometers. The chemical shifts of ^{1}H and ^{13}C are reported in ppm relative to the solvent residual peaks. Solvent peaks were used as reference values, with $CDCl_3$ at 7.26 ppm for ^{1}H NMR and 77.16 ppm for ^{13}C NMR, with $(CD_3)_2CO$ at 2.05 ppm for ^{1}H NMR and 29.84 ppm for ^{13}C NMR, and with DMSO-d_6 at 2.50 ppm for ^{1}H NMR and 39.5 ppm for ^{13}C NMR. The following abbreviations are used: singlet (s), doublet (d), doublet of doublet (dd), triplet (t), td (triplet of doublet), ddd (doublet of doublet of doublet) multiplet (m) and broad singlet (bs). IR spectra were measured on a Perkin Elmer spectrophotometer. High resolution mass spectra (HR-MS) were recorded on a MicroMass LCT Premier Spectrometer.

4.2. Chemistry

*4.2.1. General procedure for the Suzuki-Miyaura Coupling (**Method A**): compounds **14, 24, 25, 33, 41, 45, 46, 49 and 50.***

A sealed tube under argon atmosphere was charged at room temperature with ArX (0.8 mmol) and 1.5 equivalents of boronic acid (1.2 mmol). [Pd] (5 mol%), ligand (10 mol%), and base (2.4 mmol) were then added. 5 mL of the solvent were added via syringe at room temperature. The sealed tube was put into a preheated oil bath (110°C) and stirred overnight. Reaction completion was evaluated by silica TLC (80/20 cyclohexane/EtOAc). The crude mixture was then allowed to cool down to room temperature. EtOAc was added to the mixture, which was filtered through Celite. The solvents were evaporated under reduced pressure and the crude residue was purified by silica gel chromatography (95/5 to 85/15 of cyclohexane/EtOAc). The product was then concentrated under vacuum to give the desired product.

*4.2.1.1. 1-(3',4',5'-Trimethoxy-[1,1'-biphenyl]-3-yl)ethan-1-one **14***

14 was prepared according to the general method A from 5-bromo-1,2,3-trimethoxybenzene (**13**) and 3-acetylphenyl-boronic acid, using the following catalytic system: $Pd(OAc)_2$ (5 mol%), SPhos (10 mol%), $K_3PO_4.H_2O$ (3 equiv), CPME/H_2O (5:1 V/V). Column chromatography on silica gel afforded 209 mg of the product as a white powder (0.73 mmol, yield 91%); TLC (SiO_2, 80/20 cyclohexane/EtOAc); R_f = 0.28; ^{1}H NMR (300 MHz, $CDCl_3$) δ 8.13 (s, 1H, H_{Ar}), 7.92 (d, J = 7.8 Hz, 1H, H_{Ar}), 7.75 (d, J = 7.7 Hz, 1H, H_{Ar}), 7.53 (t, J = 7.7 Hz, 1H, H_{Ar}), 6.79 (s, 2H, H_{Ar}), 3.94 (s, 6H, 2 OCH_3), 3.90 (s, 3H, OCH_3), 2.66 (s, 3H, OCH_3); ^{13}C NMR (75 MHz, $CDCl_3$) δ 198.0, 153.6 (2C), 141.9, 137.6, 136.1, 131.7, 129.0 (2CH), 127.3, 126.7, 104.6 (2C), 60.1, 56.3 (2C), 26.8; HRMS (ESI+) calcd for $C_{17}H_{19}O_4$ $[M + H]^+$ 287.1278 found 287.1280.

*4.2.1.2. 4-(3-Acetylphenyl)quinoline-2-carbonitrile **24***

24 was prepared according to the general method A from 4-chloroquinoline-2-carbonitrile (**22**) and 3-acetylphenyl-boronic acid, using the following catalytic system: $Pd(PPh_3)_4$ (5 mol%), $K_3PO_4.H_2O$ (3 equiv), dioxane/H_2O (5:1 V/V). The crude residue was purified by silica gel chromatography (95/5 to 85/15 of cyclohexane/ EtOAc). Column chromatography on silica gel afforded 146 mg of the desired compound as a white solid (0.54 mmol, yield 67%). TLC (SiO_2, 80/20 cyclohexane/EtOAc) R_f = 071; m.p = 191-193 °C; ^{1}H NMR (300 MHz, $CDCl_3$) δ 8.26 (d, J = 8.0 Hz, 1H, H_{Ar}), 8.17 – 8.11 (m, 1H, H_{Ar}), 8.09 (t, J = 1.0 Hz, 1H, H_{Ar}), 7.87 (t, J = 7.8 Hz, 2H, H_{Ar}), 7.72 – 7.67 (m, 3H, H_{Ar}), 7.66 (s, 1H, H_{Ar}), 2.68 (s, 3H, CH_3); ^{13}C NMR (75 MHz, $CDCl_3$) δ 197.3, 149.4, 143.1, 137.9, 137.0, 133.9, 133.6, 131.3, 130.8, 129.5, 129.2 (2C), 129.1, 125.6, 123.6, 119.9, 117.6, 26.9; IR (ν_{max}/cm^{-1}) 3006, 2924, 2235, 1686, 1575, 1361, 1259; HRMS (ESI+) for $C_{18}H_{13}N_2O$ $[M + H]^+$: calcd 273.1028 found 273.1023.

*4.2.1.3. 1-(3-(2-Methylquinolin-4-yl)phenyl)ethan-1-one **25***

25 was prepared according to the general method A from 4-chloro-2-methylquinoline (**23**) and 3-acetylphenyl-boronic acid, using the following catalytic system: $Pd(PPh_3)_4$ (5 mol%), $K_3PO_4.H_2O$ (3 equiv), dioxane/H_2O (5:1 V/V). Column chromatography on silica gel afforded 146 mg of the desired compound as a white powder (0.56 mmol, yield 70%); TLC (SiO_2, 85/15 cyclohexane/ EtOAc) R_f = 0.15; m.p. = 125-126°C; ^{1}H NMR (300 MHz, $CDCl_3$) δ 8.18 – 8.02 (m, 3H, H_{Ar}), 7.84 – 7.55 (m, 4H, H_{Ar}), 7.45 (t, J = 7.5 Hz, 1H, H_{Ar}), 7.25 (s, 1H, H_{Ar}), 2.79 (s, 3H, CH_3), 2.66 (s, 3H, CH_3); ^{13}C NMR (75 MHz, $CDCl_3$) δ 198.2, 159.1, 149.0, 147.9, 139.3, 138.1, 134.6, 130.1, 129.8, 129.4, 128.8, 126.6, 125.7, 125.4, 122.8, 77.2, 27.3, 25.9; IR (ν_{max}/cm^{-1}) 3059, 2363, 1682, 1575, 1402, 1259, 122; HRMS (ESI+) for $C_{18}H_{16}NO$ $[M + H]^+$: calcd 262.1632, found 262.1636.

*4.2.1.4. 1-(6-(3,4,5-Trimethoxyphenyl)pyridin-2-yl)ethan-1-one **33***

33 was prepared according to the general method A from 3,4,5-trimethoxyphenyl)boronic acid (**32)** and 1-(6-bromopyridin-2-yl)ethanone, using the following catalytic system: $Pd(OAc)_2$ (5 mol%), PPh_3 (10 mol%), K_2CO_3 (3 equiv), dioxane/H_2O (5:1 V/V). Column chromatography on silica gel afforded 225 mg of the desired compound as a white solid (0.784 mmol, yield 98%). TLC (SiO_2, 85/15 cyclohexane/ EtOAc) R_f = 0.60; m.p. = 91-93 °C; ^{1}H NMR (300 MHz, $CDCl_3$) δ 7.98 – 7.92 (m, 1H ,H_{Ar}), 7.87 (dd, J = 4.6, 1.3 Hz, 2H, H_{Ar}), 7.35 (s, 2H, H_{Ar}), 3.98 (s, 6H, 2 OCH_3), 3.92 (s, 3H, OCH_3), 2.82 (s, 3H, CH_3); ^{13}C NMR (75 MHz, $CDCl_3$) δ 184.2, 156.7, 155.4, 154.2 (2C), 153.1, 138.2, 134.6, 123.8, 120.2, 105.0 (2C), 61.5, 56.9 (2C), 26.2; IR (ν_{max}/cm^{-1}) 2939, 1731, 1507, 1459, 1427, 1341, 1248, 1125, 993; HRMS (ESI+) for $C_{16}H_{18}NO_4$ $[M + H]^+$: calcd 288.1236, found 288.1234.

*4.2.1.5. 2-Methyl-4-(6-(1-(2-nitrophenyl)vinyl)pyridin-2-yl)quinoline **41***

41 was prepared according to the general method A from 2-bromo-6-(1-(2-nitrophenyl)vinyl)pyridine (**40**) and 2-methylquinolin-4-yl)boronic acid, using the following catalytic system: $Pd_2dba_3.CHCl_3$ (10 mol%), SPhos (20 mol%), K_2CO_3 (3 equiv), dioxane/H_2O (5:1 V/V). Column chromatography on silica gel afforded 88 mg of the desired compound as an orange/pink oil (0.24 mmol, yield 30%). TLC (SiO_2, 7/3 cyclohexane/AcOEt) R_f = 0.75; ^{1}H NMR (400 MHz, $CDCl_3$) δ 8.08 – 7.98 (m, 2H, H_{Ar}), 7.97 – 7.93 (m, 1H, H_{Ar}), 7.76 (t, J = 7.8 Hz, 1H, H_{Ar}), 7.61 (dtd, J = 16.3, 7.2, 1.3 Hz, 2H, H_{Ar}), 7.51 – 7.40 (m, 4H, H_{Ar}), 7.36 (ddd, J = 8.2, 7.0, 1.1 Hz, 1H, H_{Ar}), 7.33 (s, 1H, H_{Ar}), 6.34 (s, 1H, CH_2), 5.60 (s, 1H, CH_2), 2.75 (s, 3H, CH_3); ^{13}C NMR (101 MHz, $CDCl_3$) δ 158.8, 156.6, 156.3, 149.1, 148.9, 147.0, 146.3, 137.6, 136.4, 133.7, 133.0, 129.5, 129.3, 129.1, 126.2, 125.9, 124.7, 124.7, 125.0, 122.8, 120.2, 119.1, 25.7; IR (ν_{max}/cm^{-1}) 3061, 2960, 2924, 2853, 2367, 1566, 1523, 1453, 1346; HRMS (ESI+) for $C_{23}H_{18}N_3O_2$ [M + H]+: calcd 368.1399, found 368.1389.

*4.2.1.6. 3'-Bromo-4-methoxy-[1,1'-biphenyl]-3-yl acetate **45.***

45 was prepared from commercial (3-bromophenyl)boronic acid (**44)** and 5-iodo-2-methoxyphenyl acetate according to the general method A using the following catalytic system: $Pd(PPh_3)_4$ (2 mol%),

K_2CO_3 (3 equiv), toluene/H_2O (4:1 V/V). Column chromatography on silica gel afforded 158 mg of the desired compound **45** as a white solid (0.5 mmol, yield 30%). TLC (SiO_2, 7/3 cyclohexane/AcOEt) R_f = 0.47; ^{1}H NMR (300 MHz, $CDCl_3$) *δ* 7.68 (t, *J* = 1.9 Hz, 1H), 7.49 – 7.42 (m, 2H), 7.42 – 7.37 (m, 1H), 7.28 (d, *J* = 8.1 Hz, 1H), 7.25 (d, *J* = 4.1 Hz, 1H), 7.03 (d, *J* = 8.6 Hz, 1H), 3.88 (s, 3H), 2.34 (s, 3H). ^{13}C NMR (101 MHz, $CDCl_3$) δ 169.0, 151.1, 142.1, 140.2, 132.7, 130.4, 130.0, 129.9, 125.4 (2C), 123.0, 121.7, 112.8, 56.1, 20.7.

*4.2.1.7. 3'',4,4'',5''-Tetramethoxy-[1,1':3',1''-terphenyl]-3-yl acetate **46***

46 was prepared from the product 3'-bromo-4-methoxy-[1,1'-biphenyl]-3-yl acetate (**45)** and (3,4,5-trimethoxyphenyl)boronic acid **(30)** according to the general method A using the following catalytic system: $Pd(PPh_3)_4$ (2 mol%), K_2CO_3 (3 equiv), toluene/H_2O (4:1 V/V) to afforded 3'',4,4'',5''-tetramethoxy-[1,1':3',1''-terphenyl]-3-yl acetate. Column chromatography on silica gel afforded 30 mg of the desired compound **46** as a pale oil (0.07 mmol, yield 46%). TLC (SiO_2, 5/5 cyclohexane/AcOEt) R_f = 0.38; ^{1}H NMR (200 MHz, $CDCl_3$) δ 7.68 (s, 1H, H_{Ar}), 7.54 – 7.43 (m, 4H, H_{Ar}), 7.33 (d, *J* = 2.2 Hz, 1H, H_{Ar}), 7.07 (d, *J* = 8.5 Hz, 1H, H_{Ar}), 6.81 (s, 2H, H_{Ar}), 3.94 (s, 6H, 2 OCH_3), 3.91 (s, 3H, OCH_3), 3.89 (s, 3H, OCH_3), 2.35 (s, 3H, CH_3); ^{13}C NMR (75 MHz, DMSO) δ 168.5, 153.2, 150.5, 146.8, 141.2, 139.7, 139.5, 137.3, 136.1, 132.8, 129.2, 125.7, 125.2, 125.1, 124.7, 121.3, 113.1, 104.6 (2C), 60.0, 56.0 (2C), 55.9 , 20.4.

*4.2.1.8. 3'',4,4'',5''-Tetramethoxy-[1,1':3',1''-terphenyl]-3-ol **47**[35]*

Deprotection of acetate group of 3'',4,4'',5''-tetramethoxy-[1,1':3',1''-terphenyl]-3-yl acetate (**46**) with K_2CO_3 (10 eq) in MeOH afforded 3'',4,4'',5''-tetramethoxy-[1,1':3',1''-terphenyl]-3-ol (**47**). Column chromatography on silica gel afforded 16 mg of the desired compound **42** as a white beige solid (0.04 mmol, yield 73%). ^{1}H NMR (300 MHz, $CDCl_3$) *δ* 7.63 (br s, 1H, H_{Ar}), 7.48 – 7.36 (m, 3H, H_{Ar}), 7.18 (d, *J* = 2.0 Hz, 1H, H_{Ar}), 7.06 (dd, *J* = 8.3, 2.2 Hz, 1H, H_{Ar}), 6.87 (d, *J* = 8.3 Hz, 1H, H_{Ar}), 6.74 (s, 2H, H_{Ar}), 5.62 (s, 1H, OH), 3.86 (s, 3H, OCH_3), 3.86 (s, 6H, 2 OCH_3), 3.83 (s, 3H, OCH_3); ^{13}C NMR (75 MHz, $CDCl_3$) *δ* 153.5 (2C), 146.3, 145.9, 141.9, 141.3, 137.8, 137.3, 134.7, 129.1, 125.8, 125.7 (2CH), 118.9, 113.5, 111.0, 104.7 (2C), 61.0, 56.3 (2C), 56.1; HRMS (ESI+) for $C_{22}H_{23}O_5$ $[M + H]^+$: calcd 367.1545, found 367.1547.

*4.2.1.9. 2-Bromo-6-(3,4,5-trimethoxyphenyl)pyridine **49**[25]*

49 was prepared in three steep from commercial 2,6-dibromopyridine (**48**) and (3,4,5-trimethoxyphenyl)boronic acid (**30**) according to the general method A using the following catalytic system: $Pd(OAc)_2$ (5 mol%), $P(Cy_3).BF_3$ (10 mol%), K_2CO_3 (3 equiv), toluene/H_2O (30:1 V/V). Column chromatography on silica gel afforded 35 mg of the desired compound **48** as a brown solid (0.1 mmol, yield 30%). TLC (SiO_2, 7/3 cyclohexane/AcOEt) R_f = 0.53; ^{1}H NMR (300 MHz, $CDCl_3$) δ 7.66 – 7.60 (m, 1H, H_{Ar}), 7.56 (t, *J* = 7.6 Hz, 1H, H_{Ar}), 7.40 – 7.36 (m, 1H, H_{Ar}), 7.20 (s, 2H, H_{Ar}), 3.95 (s, 6H, 2 OCH_3), 3.89 (s, 3H, OCH_3).

*4.2.1.10. 2-(3-(Benzyloxy)-4-methoxyphenyl)-6-(3,4,5-trimethoxyphenyl)pyridine **50***

50 was prepared from 2-bromo-6-(3,4,5-trimethoxyphenyl)pyridine (**49**) and (3-(benzyloxy)-4-methoxyphenyl)boronic acid according to the general method A using the following catalytic system:

$Pd(OAc)_2$ (5 mol%), PPh_3 (10 mol%), K_2CO_3 (3 equiv), dioxane/H_2O (2:1 V/V) . Column chromatography on silica gel afforded 50 mg of the desired compound **49** as a pale white oil (0.11 mmol, yield 60%). TLC (SiO_2, 7/3 cyclohexane/AcOEt) R_f = 0.51; ^{1}H NMR (200 MHz, $CDCl_3$) δ 7.85 (d, *J* = 2.1 Hz, 1H, H_{Ar}), 7.78 (d, *J* = 7.8 Hz, 1H, H_{Ar}), 7.71 (dd, *J* = 8.2, 2.3 Hz, 1H, H_{Ar}), 7.59 (d, *J* = 2.2 Hz, 1H, H_{Ar}), 7.55 (dd, *J* = 2.8, 0.9 Hz, 1H, H_{Ar}), 7.53 – 7.45 (m, 2H, H_{Ar}), 7.44 – 7.31 (m, 5H, H_{Ar}), 7.02 (d, *J* = 8.5 Hz, 1H, H_{Ar}), 5.26 (s, 2H, CH_2), 3.97 (s, 6H, 2 OCH_3), 3.95 (s, 3H, OCH_3), 3.92 (s, 3H, OCH_3). ^{13}C NMR (101 MHz, CDCl3) δ 156.1, 156.0, 153.3 (2C), 150.8, 148.3, 137.4 (2C), 137.0, 128.4 (2C), 127.7, 127.2 (2C), 120.2, 117.9 (2C), 112.9 (2C), 111.7 (2C), 104.4, 104.3, 71.0, 60.8, 56.1 (2C), 55.9.

*4.2.1.11. 2-Methoxy-5-(6-(3,4,5-trimethoxyphenyl)pyridin-2-yl)phenol **8**[25]*

Deprotection of *O*-benzyl group of 2-(3-(benzyloxy)-4-methoxyphenyl)-6-(3,4,5-trimethoxyphenyl)pyridine (**50**) with Pd/C (10 mol%), H_2, in EtOH. Column chromatography on silica gel afforded 20 mg of the desired compound **8** as a white solid (0.05 mmol, yield 80%). ^{1}H NMR (300 MHz, $CDCl_3$) δ 7.83 – 7.72 (m, 2H, H_{Ar}), 7.67 (dd, *J* = 8.4, 2.2 Hz, 1H, H_{Ar}), 7.59 (ddd, *J* = 7.6, 6.5, 0.9 Hz, 2H, H_{Ar}), 7.37 (s, 2H, H_{Ar}), 6.97 (d, *J* = 8.4 Hz, 1H, H_{Ar}), 5.71 (s, 1H, OH), 3.99 (s, 6H, 2 OCH_3), 3.96 (s, 3H, OCH_3), 3.91 (s, 3H, OCH_3); ^{13}C NMR (101 MHz, $CDCl_3$) δ 156.5, 156.4, 153.6 (2C), 147.7, 145.9, 139.3, 137.5, 135.5, 133.2, 119.1, 118.1 (2C), 113.3, 110.8, 104.6 (2C), 61.1, 56.5 (2C), 56.2; HRMS (ESI+) for $C_{21}H_{22}NO_5$ $[M + H]^+$: calcd 368.1498, found 368.1502.

*4.2.3. General procedure for the preparation of N-tosylhydrazones derivatives (**Method B**): **15, 26, 27, 34** and **39***

A round bottom flask was charged with 1 equivalent of ketone and 2 equivalents of 4-methylbenzenesulfonohydrazide in 15mL of absolute ethanol was refluxed for 16 h at 95°C. Reaction completion was evaluated by silica TLC (85/15 cyclohexane/AcOEt). The crude mixture was then allowed to cool down to room temperature and put in an ice bath to form a solid which was filtered with absolute ethanol to give the product as a solid.

*4.2.3.1. (E)-4-Methyl-N'-(1-(3',4',5'-trimethoxy-[1,1'-biphenyl]-3yl)ethylidene)benzenesulfonohydrazide **15***

15 was prepared according to the general method B from 1-(3',4',5'-trimethoxy-[1,1'-biphenyl]-3-yl) ethan-1-one (4 mmol) (**15**) and 4-methylbenzenesulfonohydrazide (8 mmol). Crystallization in cold bath and then filtration afforded 1.55 g of the product as an orange solid (3.43 mmol, yield 86%); TLC (SiO_2, 8/2 cyclohexane/EtOAc) R_f = 0.59; m.p. = 173-175 °C; ^{1}H NMR (300 MHz, $CDCl_3$) δ 7.92 (d, *J* = 8.2 Hz, 2H, H_{Ar}), 7.79 (s, 1H, H_{Ar}), 7.61 (d, *J* = 7.6 Hz, 1H, H_{Ar}), 7.54 (d, *J* = 7.6 Hz, 1H, H_{Ar}), 7.47 (s, 1H, H_{Ar}), 7.41 (t, *J* = 7.7 Hz, 1H, H_{Ar}), 7.31 (d, *J* = 8.1 Hz, 2H, H_{Ar}), 6.75 (s, 2H, H_{Ar}), 3.94 (s, 6H, 2OCH_3), 3.91 (s, 3H, OCH_3), 2.41 (s, 3H, CH_3), 2.20 (s, 3H, CH_3); ^{13}C NMR (75 MHz, $CDCl_3$) δ 154.1, 153.0 (2C), 144.8, 142.1 (2C), 138.4, 137.4, 136.0, 130.1 (2C), 129.3 (2C), 128.9, 128.74, 125.8, 125.7, 105.2 (2C), 61.56, 56.87 (2C), 22.17, 14.16; HRMS (ESI+) for $C_{24}H_{27}N_2O_5S$ $[M + H]^+$: calcd 455.1635, found 455.1673.

*4.2.3.2. (E)-N'-(1-(3-(2-Cyanoquinolin-4-yl)phenyl)ethylidene)-4-methylbenzenesulfonohydrazide **26***

26 was prepared according to the general method B from 4-(3-acetylphenyl)quinoline-2-carbonitrile (**24**) (1.9 mmol) and 4-methylbenzenesulfonohydrazide (3.86 mmol). Crystallization in cold bath and then filtration afforded 510 mg of the desired compound as a yellow powder (1.16 mmol, yield 60%). TLC (SiO_2, 6/4 cyclohexane/EtOAc) R_f = 0.62; m.p. = 182-184 °C; ^{1}H NMR (300 MHz, $CDCl_3$) δ 8.26 (d, *J*

= 8.4 Hz, 1H, H_{Ar}), 7.92 (d, *J* = 8.9 Hz, 2H, H_{Ar}), 7.88 – 7.83 (m, 3H, H_{Ar}), 7.80 (dt, *J* = 7.7, 1.6 Hz, 1H, H_{Ar}), 7.75 (d, *J* = 1.8 Hz, 1H, H_{Ar}), 7.67 (ddd, *J* = 8.4, 6.9, 1.3 Hz, 1H, H_{Ar}), 7.60 (s, 1H, H_{Ar}), 7.56 (t, *J* = 7.7 Hz, 1H, H_{Ar}), 7.49 (dd, *J* = 7.7, 1.5 Hz, 1H, H_{Ar}), 7.24 (s, 1H, H_{Ar}), 2.39 (s, 3H, CH_3), 2.22 (s, 3H, CH_3); ^{13}C NMR (75 MHz, $CDCl_3$) δ 151.5, 150.0, 149.0, 144.6, 138.3, 136.6, 135.4, 133.5, 131.2, 130.7, 130.5, 129.7 (2C), 129.2, 128.3 (2C), 128.1, 127.5, 127.4, 127.2, 125.91, 123.2, 117.8, 21.7, 13.6. IR (ν_{max}/cm^{-1}) 3242, 3063, 2925, 2360, 1597, 1405, 1335, 1167, 1066; HRMS (ESI+) for $C_{25}H_{20}N_4O_2S$ [M + H]$^+$: calcd 441.1385, found 441.1385.

*4.2.3.3. (E)-4-Methyl-N'-(1-(3-(2-methylquinolin-4-yl)phenyl)ethylidene)benzenesulfonohydrazide **27***

27 was prepared according to the general method B from 1-(3-(2-methylquinolin-4-yl)phenyl)ethan-1-one (**25)** (2.30 mmol) and 4-methylbenzenesulfonohydrazide (4.6 mmol)**.** Crystallization in cold bath and then filtration afforded 909 mg of the desired compound as a white solid (2.12 mmol, yield 92%). TLC (SiO_2, 6/4 cyclohexane/ EtOAc) R_f = 0.29; m.p. = 144-146 °C; ^{1}H NMR (300 MHz, $CDCl_3$) δ 8.17 (d, *J* = 8.5 Hz, 1H, H_{Ar}), 7.88 (d, *J* = 8.2 Hz, 2H, H_{Ar}), 7.79 (d, *J* = 8.0 Hz, 2H, H_{Ar}), 7.74 (s, 2H, H_{Ar}), 7.49 (p, *J* = 7.8 Hz, 3H, H_{Ar}), 7.23 (d, *J* = 5.3 Hz, 2H, H_{Ar}), 7.19 (s, 1H, H_{Ar}), 2.83 (s, 3H, CH_3), 2.36 (s, 3H, CH_3), 2.20 (s, 3H, CH_3); ^{13}C NMR (75 MHz, $CDCl_3$) δ 158.3, 151.8, 146.0, 144.9, 144.2, 138.0, 137.8, 135.3, 131.3, 130.5, 129.8, 129.5 (2C), 128.7, 128.2 (2C), 127.4, 126.4, 126.2, 125.5, 125.0, 122.2, 24.9, 21.6, 13.5; IR (ν_{max}/cm^{-1}) 2360, 2252, 1686, 1403, 1339, 1302, 1165, 905; HRMS (ESI+) for $C_{25}H_{23}N_3O_2S$ [M + H]$^+$: calcd 430.1589, found 430.1581.

*4.2.3.4. (E)-4-Methyl-N'-(1-(6-(3,4,5-trimethoxyphenyl)pyridin-2yl)ethylidene)benzenesulfonohydrazide **34***

34 was prepared according to the general method B from 1-(6-(3,4,5-trimethoxyphenyl)pyridin-2-yl)ethan-1-one (**33)** (1.38 mmol) and 4-methylbenzenesulfonohydrazide (2.77 mmol)**.** Crystallization in cold bath and then filtration afforded 440 mg of the desired compound as an orange solid (0.97 mmol, yield 70%). TLC (SiO_2, 60/40 cyclohexane/EtOAc) R_f = 0.60; m.p. = 186-187 °C; ^{1}H NMR (400 MHz, $CDCl_3$) δ 14.98 (s, 1H, NH), 8.03 (t, *J* = 8.0 Hz, 1H, H_{Ar}), 7.96 (d, *J* = 8.3 Hz, 2H, H_{Ar}), 7.86 (d, *J* = 8.0 Hz, 1H, H_{Ar}), 7.52 (d, *J* = 7.9 Hz, 1H, H_{Ar}), 7.39 (d, *J* = 8.5 Hz, 2H, H_{Ar}), 7.26 (s, 2H, H_{Ar}), 4.15 (s, 6H, 2 OCH_3), 4.07 (s, 3H, OCH_3), 2.51 (s, 3H, CH_3), 2.47 (s, 3H, CH_3); ^{13}C NMR (101 MHz, $CDCl_3$) δ 155.9, 154.0, 152.9, 143.5, 141.5, 140.0, 138.7, 137.1, 136.8, 133.4, 129.5, 128.1, 127.6, 121.9, 121.5, 120.2, 118.9, 104.3, 104.3, 61.0, 56.5, 22.5, 21.6; IR (ν_{max}/cm^{-1}) 2996, 2943, 2359, 1574, 1507, 1462, 1403, 1344, 1159, 1126, 1080, 1033; HRMS (ESI+) for $C_{23}H_{26}N_3O_5S$ [M + H]$^+$: calcd 456.1593, found 456.1586.

*4.2.3.5. (E)-N'-(1-(6-Bromopyridin-2-yl)ethylidene)-4-methylbenzenesulfonohydrazide **39***

39 was prepared according to the general method B from 1-(6-bromopyridin-2-yl)ethan-1-one (**38**) (1.24 mmol) and 4-methylbenzenesulfonohydrazide (2.48 mmol). Crystallization in cold bath and then filtration 380 mg of the desired compound as a white powder (1,03 mmol, yield 83%). TLC (SiO_2, 8/2 cyclohexane/EtOAc) R_f = 0.74; m.p. = 230-231 °C; ^{1}H NMR (300 MHz, DMSO-d_6) δ 10.92 (s, 1H, NH), 7.85 – 7.78 (m, 3H, H_{Ar}), 7.75 (td, *J* = 7.6, 0.9 Hz, 1H, H_{Ar}), 7.62 (dt, *J* = 7.4, 1.1 Hz, 1H, H_{Ar}), 7.41 (d, *J* = 8.0 Hz, 2H, H_{Ar}), 2.37 (s, 3H, CH_3), 2.19 (s, 3H, CH_3); ^{13}C NMR (75 MHz, DMSO-d_6) δ 155.7, 151.4, 143.5, 140.2, 139.9, 136.0, 129.5 (2C), 128.2, 127.5 (2C), 119.1, 21.0, 12.5. IR (ν_{max}/cm^{-1}) 3225, 2425,

2412, 1675, 1610, 1480, 1375, 1212; HRMS (ESI+) for $C_{14}H_{15}N_3O_2SBr$ $[M + H]^+$: calcd 368.0068, found 368.0067.

*4.2.4. General procedure for the Barluenga coupling followed Cadogan cyclisation one pot (**Method C**): **16-19, 28, 29, 35, and 42***

A sealed tube under argon atmosphere was charged at room temperature with 1 equivalent of corresponding *N*-tosylhydrazone (0.2 mmol), 1 equivalent of appropriate 1-bromo-2-nitrobenzene derivative (0.2 mmol), $Pd_2dba_3.CHCl_3$ (5 mol%), XPhos (10 mol%) and 2.5 equivalent of Li*O*t*B*u (0.5 mmol) in dry dioxane. The mixture was then heated at 110 °C for 16h. Reaction completion was evaluated by silica TLC (8/2 cyclohexane/AcOEt). The crude mixture was then allowed to cool down to room temperature, Filtration through Celite, and evaporation to give an oily brown crude directly used for next step without purification. In a sealed tube the 1-nitro-2-(1-phenylvinyl)benzene derivative was treated with 4 equivalent of PPh_3 and 10 mol% of catalyst $MoO_2Cl_2(DMF)_2$ in 2mL of dry dioxane under argon and stirred in MW at 135 °C for 4h. The crude mixture was then allowed to cool down to room temperature. EtOAc was added to the mixture, which was filtered through Celite. The solvents were evaporated under reduced pressure and the crude residue was purified by silica gel chromatography (95/5 to 85/15 of cyclohexane/EtOAc). The product was then concentrated under vacuum to give the product as a white solid.

*4.2.4.1. 3-(3',4',5'-Trimethoxy-[1,1'-biphenyl]-3-yl)-1H-indole **16***

16 was prepared according to the general method C from (**15**) and 1-bromo-2-nitrobenzene. Column chromatography on silica gel afforded 40 mg of the product as an orange solid (0.11 mmol, yield 55%); TLC (SiO_2, 8/2 cyclohexane/EtOAc) R_f = 0.23; m.p. = 170-172 °C; ^{1}H NMR (300 MHz, $CDCl_3$) δ 8.40 (brs, 1H, NH), 7.98 (d, J = 7.7 Hz, 1H, H_{Ar}), 7.86 (s, 1H, H_{Ar}), 7.67 (d, J = 7.1 Hz, 1H, H_{Ar}), 7.54 (d, J = 7.6 Hz, 1H, H_{Ar}), 7.49 (d, J = 7.6 Hz, 2H, H_{Ar}), 7.44 (d, J = 5.4 Hz, 1H, H_{Ar}), 7.30 (d, J = 7.2 Hz, 1H, H_{Ar}), 7.25 – 7.18 (m, 1H, H_{Ar}), 6.87 (s, 2H, H_{Ar}), 3.95 (s, 6H, 2 OCH_3), 3.93 (s, 3H, OCH_3); ^{13}C NMR (75 MHz, $CDCl_3$) δ 153.5, 142.0, 137.5, 136.7, 136.1, 129.2, 126.6, 126.3, 125.8, 124.9, 122.5, 122.0, 120.4, 119.7, 118.2, 111.5, 104.6, 61.0, 56.2. IR (ν_{max}/cm^{-1}) 2938, 1582, 1511, 1455, 1238, 1126, 1002; HRMS (ESI^+) for $C_{23}H_{22}NO_3$ $[M + H]^+$ calcd 360.1594 found 360.1653; LCMS 97% 20.2 min.

*4.2.4.2. 6-Methoxy-3-(3',4',5'-trimethoxy-[1,1'-biphenyl]-3-yl)-1H-indole **17***

17 was prepared according to the general method C from (**15**) and 1-bromo-4-methoxy-2-nitrobenzene. Column chromatography on silica gel afforded 27 mg of the product as a yellow oil (0.07 mmol, yield 35%); TLC (SiO_2, 80/20 cyclohexane/AcOEt) R_f = 0.6; ^{1}H NMR (300 MHz, $CDCl_3$) δ 8.27 (brs, 1H, NH), 7.89 – 7.77 (m, 2H, H_{Ar}), 7.64 (dt, J = 7.0, 1.5 Hz, 1H, H_{Ar}), 7.57 – 7.42 (m, 2H, H_{Ar}), 7.32 (d, J = 2.4 Hz, 1H, H_{Ar}), 6.93 (d, J = 2.1 Hz, 1H, H_{Ar}), 6.92 – 6.81 (m, 3H, H_{Ar}), 3.94 (s, 6H, 2 OCH_3), 3.93 (s, 3H, OCH_3), 3.87 (s, 3H, OCH_3); ^{13}C NMR (75 MHz, $CDCl_3$) δ 156.3, 153.2 (2C), 141.7, 137.8, 137.7, 136.4, 135.7, 129.0, 126.2, 125.9, 124.4, 121.2, 120.0, 118.8, 117.3, 109.9, 104.5 (2C), 95.0, 60.8, 56.1 (2C), 55.6; IR (ν_{max}/cm^{-1}) 2925, 1581, 1455, 1240, 1164, 1125, 1003; HRMS (ESI+) for $C_{24}H_{24}NO_4$ $[M + H]^+$ calcd 390.1700 found 390.1731; LCMS 95% 19,9 min.

*4.2.4.3. 3-(3',4',5'-Trimethoxy-[1,1'-biphenyl]-3-yl)-1H-indole-6-carbonitrile **18***

18 was prepared according to the general method C from (**15**) and 4-bromo-3-nitrobenzonitrile. Column chromatography on silica gel afforded 16 mg of the product as a viscous yellow liquid (0.04 mmol; yield 20%); TLC (SiO_2, 80/20 cyclohexane/AcOEt) R_f = 0.6; ^{1}H NMR (300 MHz, $CDCl_3$) δ 8.81 (brs, 1H, NH), 7.99 (d, *J* = 8.4 Hz, 1H, H_{Ar}), 7.83 – 7.75 (m, 2H, H_{Ar}), 7.63 (d, *J* = 2.7 Hz, 1H, H_{Ar}), 7.61 – 7.56 (m, 1H, H_{Ar}), 7.55 – 7.50 (m, 2H, H_{Ar}), 7.43 (dd, *J* = 8.4, 1.3 Hz, 1H, H_{Ar}), 6.65 (s, 2H, H_{Ar}), 3.94 (s, 6H, 2 OCH_3), 3.92 (s, 3H, OCH_3); ^{13}C NMR (75 MHz, $CDCl_3$)) δ 153.5 (2C), 142.3, 137.2, 134.6 (2C), 129.4, 128.9, 126.7, 126.4 (2C), 125.6 (2C), 123.3, 120.6, 120.4, 116.4, 115.9, 105.1, 104.7 (2C), 61.0, 56.3 (2C); IR (ν_{max}/cm^{-1}) 2924, 2222, 1602, 1462, 1399, 1265, 1128, 1029; HRMS (ESI$^+$) for $C_{24}H_{21}N_2O_3$ $[M + H]^+$: calcd 385.1547 found 385.1505; LCMS 96% 19.7 min.

*4.2.4.4. 6-(Trifluoromethyl)-3-(3',4',5'-trimethoxy-[1,1'-biphenyl]-3-yl)-1H-indole **19***

19 was prepared according to the general method C from (**15**) and 1-bromo-2-nitro-4-(trifluoromethyl)benzene. Column chromatography on silica gel afforded 22 mg of the product as a white solid (0.05 mmol, yield 26%); TLC (SiO_2, 80/20 cyclohexane/ EtOAc) Rf = 0.15; m.p. = 180-182 °C; ^{1}H NMR (300 MHz, $CDCl_3$) δ 8.74 (s, 1H, NH), 8.03 (d, *J* = 8.4 Hz, 1H, H_{Ar}), 7.81 (s, 1H, H_{Ar}), 7.75 (s, 1H, H_{Ar}), 7.63 (dt, *J* = 4.0, 1.9 Hz, 1H, H_{Ar}), 7.57 (d, *J* = 2.4 Hz, 1H, H_{Ar}), 7.55 – 7.49 (m, 2H, H_{Ar}), 7.45 (s, 1H, H_{Ar}), 6.86 (s, 2H, H_{Ar}), 3.95 (s, 6H, 2 OCH_3), 3.93 (s, 3H, OCH_3); ^{13}C NMR (101 MHz, DMSO-d_6) δ 153.2 (2C), 141.2, 137.3, 136.3, 135.6, 135.4, 129.2, 127.5, 127.1, 125.7, 125.3 (q, 1C, *J* = 271.3 Hz, CF_3), 125.2, 124.5, 121.8 (q, 1C, *J* = 31.1 Hz, C), 119.9, 116.1, 115.9 (q, 1C, *J* = 4.2 Hz, CH), 109.3 (q, 1C, *J* = 4.2 Hz, CH), 104.5 (2C), 60.0, 56.0 (2C); IR (ν_{max}/cm^{-1}) 2932, 1580, 1509, 1459, 1332, 1237, 1126, 1100, 1000; ^{19}F NMR (200 MHz, $CDCl_3$) δ -60.73 (CF_3); HRMS (ESI+) for $C_{24}H_{21}F_3NO_3$ $[M + H]^+$: calcd 428.1468 found 428.1478; LCMS 100% 21,6 min.

*4.2.4.5. 4-(3-(1H-Indol-3-yl)phenyl)quinoline-2-carbonitrile **28***

28 was prepared according to the general method C from (**26**) and 1-bromo-2-nitrobenzene but with Cs_2CO_3 base instead of Li*Ot*Bu. Column chromatography on silica gel afforded 32 mg of the desired compound as a pale white solid (0.092 mmol, yield 46%). TLC (SiO_2, 70/30 cyclohexane/ EtOAc) Rf = 0.58; m.p. = 204-206 °C; ^{1}H NMR (400 MHz, DMSO-d_6) δ 11.46 (s, 1H, NH), 8.22 (dd, *J* = 8.6, 1.2 Hz, 1H, H_{Ar}), 8.11 (s, 1H, H_{Ar}), 8.09 (dd, *J* = 8.6, 1.3 Hz, 1H, H_{Ar}), 7.99 – 7.92 (m, 2H, H_{Ar}), 7.90 (dt, *J* = 7.3, 1.8 Hz, 2H, H_{Ar}), 7.84 (d, *J* = 2.4 Hz, 1H, H_{Ar}), 7.80 (ddd, *J* = 8.3, 6.9, 1.3 Hz, 1H, H_{Ar}), 7.66 (t, *J* = 7.7 Hz, 1H, H_{Ar}), 7.48 (dd, *J* = 8.0, 0.9 Hz, 1H, H_{Ar}), 7.44 (dt, *J* = 7.7, 1.4 Hz, 1H, H_{Ar}), 7.16 (ddd, *J* = 8.2, 7.0, 1.2 Hz, 1H, H_{Ar}), 7.09 (ddd, *J* = 8.2, 7.0, 1.2 Hz, 1H, H_{Ar}); ^{13}C NMR (101 MHz, DMSO-d_6) δ 150.0, 148.0, 136.9, 136.6, 136.3, 132.8, 131.3, 129.1, 129.8, 129.3, 127.4, 127.1, 126.8, 126.4, 125.8, 124.8, 124.2, 123.7, 121.5, 119.8, 118.9, 117.7, 114.9, 112.0; IR (ν_{max}/cm^{-1}) 3062, 2959, 2919, 2851, 2360, 2235,1579, 1545, 1457, 1261, 1125, 800, 768, 743; HRMS (ESI+) for $C_{24}H_{16}N_3$ $[M + H]$+: calcd 346.1344, found 346.1342; LCMS 100% 21,7 min.

*4.2.4.6. 4-(3-(1H-Indol-3-yl)phenyl)-2-methylquinoline **29***

29 was prepared according to the general method C from (**27**) and 1-bromo-2-nitrobenzene. Column chromatography on silica gel afforded 57 mg of the desired compound as a yellow solid (0.17 mmol, yield 83%). TLC (SiO_2, 5/5 cyclohexane/ EtOAc) Rf = 0.42; m.p. = 209-211 °C; ^{1}H NMR (300 MHz, DMSO-d_6) δ 11.42 (s, 1H, NH), 8.02 (d, *J* = 8.4 Hz, 1H, H_{Ar}), 7.94 (d, *J* = 8.4 Hz, 1H, H_{Ar}), 7.88 (t, *J* = 8.3

Hz, 2H, H_{Ar}), 7.81 (t, *J* = 2.6 Hz, 2H, H_{Ar}), 7.78 – 7.71 (m, 1H, H_{Ar}), 7.63 (t, *J* = 7.7 Hz, 1H, H_{Ar}), 7.57 – 7.50 (m, 1H, H_{Ar}), 7.47 (s, 1H, H_{Ar}), 7.45 (d, *J* = 8.2 Hz, 1H, H_{Ar}), 7.39 (d, *J* = 7.5 Hz, 1H, H_{Ar}), 7.16 (t, *J* = 7.5 Hz, 1H, H_{Ar}), 7.09 (t, *J* = 7.4 Hz, 1H, H_{Ar}), 2.72 (s, 3H, CH_3); ^{13}C NMR (75 MHz, DMSO-d_6) δ 158.9, 148.4, 148.2, 138.5, 137.4, 136.8, 129.8, 129.6, 129.3, 127.7, 127.0, 126.7, 126.5, 125.7, 125.4, 125.0, 124.5, 122.6, 122.0, 120.3, 119.4, 115.6, 112.5, 25.3. IR (ν_{max}/cm^{-1}) 2923, 2852, 2360, 1592, 1560, 1540, 1457, 1263, 1240, 1198, 1013, 800, 767, 739; HRMS (ESI+) for $C_{24}H_{19}N_2$ [M + H]+: calcd 335.1548, found 335.1547; LCMS 100% 14,6 min.

4.2.4.7. 3-(6-(3,4,5-Trimethoxyphenyl)pyridin-2-yl)-1H-indole ***35***

35 was prepared according to the general method C from (**34**) and 1-iodo-2-nitrobenzene. Column chromatography on silica gel afforded 41 mg of the desired compound as a pale yellow solid (0,114 mmol, yield 57%). TLC (SiO_2, 60/40 cyclohexane/ EtOAc) Rf = 0.64; m.p. = 231 – 233 °C; ^{1}H NMR (300 MHz, DMSO-d_6) δ 11.52 (s, 1H, NH), 8.71 (d, *J* = 7.4 Hz, 1H, H_{Ar}), 8.19 (s, 1H, H_{Ar}), 7.89 – 7.69 (m, 3H, H_{Ar}), 7.57 (s, 2H, H_{Ar}), 7.47 (d, *J* = 7.8 Hz, 1H, H_{Ar}), 7.24 – 7.09 (m, 2H, H_{Ar}), 3.95 (s, 6H, 2 OCH_3), 3.76 (s, 3H, OCH_3); ^{13}C NMR (101 MHz, DMSO-d_6) δ 155.0, 154.7, 153.1 (2C), 138.3, 137.1, 137.0, 134.8, 126.2, 125.4, 121.7, 121.6, 119.9, 117.8, 115.7, 115.4, 111.8, 103.8 (2CH), 60.1, 55.8 (2OCH_3); IR (ν_{max}/cm^{-1}) 3331, 3006, 2918, 2359, 1583, 1461, 1429, 1119, 1003, 808, 746; HRMS (ESI+) for $C_{22}H_{21}N_2O_3$ [M + H]+: calcd 361.1552, found 361.1556; LCMS 100% 18,17min

4.2.4.8. 2-Bromo-6-(1-(2-nitrophenyl)vinyl)pyridine ***40***

40 was prepared from (**39**) and 1-iodo-2-nitrobenzene according to the general method C. The reaction was stopped at the Barluenga coupling step. Column chromatography on silica gel afforded 33 mg of the desired compound as a white solid (0.11 mmol, yield 55%). TLC (SiO_2, 70/30 cyclohexane/EtOAc) R_f = 0.26; m.p. = 100-102 °C; ^{1}H NMR (300 MHz, $CDCl_3$) δ 8.05 (dd, *J* = 8.1, 1.3 Hz, 1H, H_{Ar}), 7.66 (td, *J* = 7.7, 1.2 Hz, 1H, H_{Ar}), 7.54 (td, *J* = 7.8, 1.6 Hz, 1H, H_{Ar}), 7.49 – 7.40 (m, 2H, H_{Ar}), 7.34 (d, *J* = 7.8 Hz, 1H, H_{Ar}), 7.14 (d, *J* = 7.6 Hz, 1H, H_{Ar}), 6.38 (s, 1H, CH_2), 5.54 (s, 1H, CH_2); ^{13}C NMR (75 MHz, $CDCl_3$) δ 157.1, 145.1, 141.8, 138.9, 135.2, 133.4, 132.7, 129.2, 129.0, 127.1, 124.6, 119.8, 119.5; IR (ν_{max}/cm^{-1}) 2959, 2924, 2853, 1573, 1550, 1520, 1433, 1383, 1121, 983; HRMS (ESI+) for $C_{13}H_{10}N_2O_2Br$ [M + H]+: calcd 304.9926, found 304.9919.

4.2.4.9. 4-(6-(1H-Indol-3-yl)pyridin-2-yl)-2-methylquinoline ***42***

Was prepared according to the general method C from (**41**). Column chromatography on silica gel afforded 50 mg of the desired compound as a yellow solid (0.15 mmol, yield 75%). TLC (SiO_2, 50/50 cyclohexane/ EtOAc) Rf = 0.62; m.p. = 223-225 °C; ^{1}H NMR (300 MHz, DMSO-d_6 δ 11.60 (brs, 1H, NH), 8.38 (d, *J* = 8.0 Hz, 1H, H_{Ar}), 8.32 (d, *J* = 8.4 Hz, 1H, H_{Ar}), 8.22 (s, 1H, H_{Ar}), 8.05 (d, *J* = 8.4 Hz, 1H, H_{Ar}), 8.00 (d, *J* = 7.8 Hz, 1H, H_{Ar}), 7.94 (t, *J* = 7.7 Hz, 1H, H_{Ar}), 7.80 – 7.71 (m, 1H, H_{Ar}), 7.61 (s, 1H, H_{Ar}), 7.55 – 7.50 (m, 1H, H_{Ar}), 7.50 – 7.43 (m, 2H, H_{Ar}), 7.13 (t, *J* = 7.7 Hz, 1H, H_{Ar}), 6.99 (t, *J* = 7.5 Hz, 1H, H_{Ar}), 2.75 (s, 3H, CH_3); ^{13}C NMR (75 MHz, DMSO-d_6) δ 158.4, 155.3, 155.3, 148.1, 146.1, 137.2, 137.0, 129.2, 128.7, 126.5, 125.8, 125.7, 125.2, 123.9, 121.9, 121.7, 121.6, 120.4, 119.1, 118.8, 115.0, 111.7, 24.8; IR (ν_{max}/cm^{-1}) 2917, 2362, 2341, 1618, 1412, 1174, 747; HRMS (ESI+) for $C_{23}H_{18}N_3$ [M + H]+: calcd 336.1501, found 336.1496; LCMS 100% 12,35min.

*4.2.5. General procedure for N-methylation of indole (****Method D****):* ***20, 30, 36*** *and* ***43***

In a round bottom flask 1 equivalent of corresponding indole was dissolved in freshly distilled DMF (1mL) at 0 °C and 2.5 equivalent of NaH was added. After 20 min, 1.2 equivalent of MeI was slowly injected and the mixture was allowed to stir at room temperature for 6 h. Reaction completion was evaluated by silica TLC (6/4 cyclohexane/EtOAc). The reaction was cooled to 0 °C, saturated aqueous NH_4Cl was added and the mixture was extracted with EtOAc. The combined organic layers were washed with $NaHCO_3$ and brine, dried over $MgSO_4$ and concentrated in vacuum. The crude product was purified by silica gel chromatography (8/2 to 6/4 cyclohexane/EtOAc).

*4.2.5.1. 1-Methyl-3-(3',4',5'-trimethoxy-[1,1'-biphenyl]-3-yl)-1H-indole **20***

20 was prepared according to the general method D from (**16**) (0.10 mmol) and MeI (0.14 mmol). Column chromatography on silica gel afforded 22 mg of the product as a viscous pale brown liquid (0.06 mmol, yield 53%); TLC (SiO_2, 80/20 cyclohexane/EtOAc) R_f = 0.29; ^{1}H NMR (300 MHz, $CDCl_3$) δ 7.94 (d, *J* = 7.9 Hz, 1H, H_{Ar}), 7.79 (s, 1H, H_{Ar}), 7.61 (d, *J* = 7.3 Hz, 1H, H_{Ar}), 7.51 – 7.41 (m, 2H, H_{Ar}), 7.41 – 7.32 (m, 1H, H_{Ar}), 7.28 (d, *J* = 7.4 Hz, 1H, H_{Ar}), 7.25 – 7.19 (m, 1H, H_{Ar}), 7.16 (d, *J* = 7.5 Hz, 1H, H_{Ar}), 6.82 (s, 2H, H_{Ar}), 3.90 (s, 6H, 2 OCH_3), 3.88 (s, 3H, NCH_3), 3.83 (s, 3H, OCH_3); ^{13}C NMR (75 MHz, $CDCl_3$) *δ* 153.5 (2C), 141.1, 140.9, 137.7, 137.5, 136.1, 129.1, 126.7, 126.4, 126.2, 124.9, 124.6, 122.1, 120.0, 119.8, 116.6, 109.6, 104.6 (2C), 61.0, 56.2 (2C), 32.9. IR (ν_{max}/cm^{-1}) 1616, 1580, 1464, 1401, 1240, 1126, 1004; HRMS (ESI+) for $C_{24}H_{24}NO_3$ $[M + H]^+$: calcd 374.1751 found 374.1717; LCMS 100% 21,6 min.

*4.2.5.2. 2-Methyl-4-(3-(1-methyl-1H-indol-3-yl)phenyl)quinoline **30***

30 was prepared according to the general method D from (**29**) (0.086 mmol) and MeI (0.1 mmol). Column chromatography on silica gel afforded 23 mg of the desired compound as a yellow solid (0.066 mmol, yield 76%). TLC (SiO_2, 5/5 cyclohexane/ EtOAc) R_f = 0.54; m.p. = 200-202 °C; ^{1}H NMR (300 MHz, $CDCl_3$) *δ* 8.03 (d, *J* = 8.5 Hz, 1H, H_{Ar}), 7.97 – 7.81 (m, 2H, H_{Ar}), 7.71 (dd, *J* = 4.1, 2.3 Hz, 2H, H_{Ar}), 7.62 (ddd, *J* = 8.4, 6.9, 1.4 Hz, 1H, H_{Ar}), 7.50 (t, *J* = 7.9 Hz, 1H, H_{Ar}), 7.37 (t, *J* = 7.6 Hz, 1H, H_{Ar}), 7.33 – 7.28 (m, 2H, H_{Ar}), 7.23 (d, *J* = 5.1 Hz, 2H, H_{Ar}), 7.20 – 7.16 (m, 1H, H_{Ar}), 7.12 (t, 1H, H_{Ar}), 3.77 (s, 3H, NCH_3), 2.72 (s, 3H, CH_3); ^{13}C NMR (75 MHz, $CDCl_3$) *δ* 169.4, 158.7, 148.9, 148.6, 138.8, 137.7, 136.2, 129.4, 129.2, 129.1, 128.4, 127.2, 127.1, 127.0, 126.2, 126.0, 125.9, 125.37, 122.34, 120.3, 120.0, 116.3, 109.8, 33.2, 25.5; IR (ν_{max}/cm^{-1}) 2961, 2919, 2850, 2362, 1596, 1483, 1379, 1334, 1260, 1096, 1014, 800, 756; HRMS (ESI+) for $C_{25}H_{21}N_2$ [M + H]+: calcd 349.1705, found 349.1712; LCMS 100% 14,3 min.

*4.2.5.3. 1-Methyl-3-(6-(3,4,5-trimethoxyphenyl)pyridin-2-yl)-1H-indole **36***

36 was prepared according to the general method D from (**35**) (0.057 mmol) and MeI (0.114 mmol). Column chromatography on silica gel afforded 16 mg of the desired compound as a yellow solid (0,04 mmol, yield 71%). TLC (SiO_2, 60/40 cyclohexane/ EtOAc) R_f = 0.55; m.p. = 109-111 °C; ^{1}H NMR (300 MHz, acetone-d_6) *δ* 8.81 (d, *J* = 7.8 Hz, 1H, H_{Ar}), 8.03 (s, 1H, H_{Ar}), 7.83 – 7.73 (m, 1H, H_{Ar}), 7.69 (ddd, *J* = 8.6, 7.7, 1.2 Hz, 2H, H_{Ar}), 7.62 (s, 2H, H_{Ar}), 7.47 (dd, *J* = 7.1, 1.8 Hz, 1H, H_{Ar}), 7.32 – 7.11 (m, 2H, H_{Ar}), 3.99 (s, 6H, 2 OCH_3), 3.93 (s, 3H, NCH_3), 3.82 (s, 3H, CH_3); ^{13}C NMR (75 MHz, acetone-d_6) *δ* 184.6, 178.6, 156.6, 156.1, 154.6, 147.7, 138.1, 137.1, 136.3, 130.5, 127.4, 123.2, 122.9, 121.1, 118.5, 116.5, 110.6, 105.2 (2C), 60.7, 56.5 (2C), 33.2; IR (ν_{max}/cm^{-1}) 2935, 2359,1582, 1542, 1505, 1445, 1421, 1334, 1215, 1124, 800, 741; HRMS (ESI+) for $C_{23}H_{23}N_2O_3$ [M + H]+: calcd 375.1709, found 375.1704; LCMS 100% 19,2 min.

*4.2.5.4. 2-Methyl-4-(6-(1-methyl-1H-indol-3-yl)pyridin-2-yl)quinoline **43***

43 was prepared according to the general method D from (**42**) (0.047 mmol) and MeI (0.093 mmol). Column chromatography on silica gel afforded 15 mg of the desired compound as a pale yellow solid (0.04 mmol, yield 86%). TLC (SiO_2, 60/40 cyclohexane/ EtOAc) R_f = 0.72; m.p. = 152-154 °C; ^{1}H NMR (400 MHz, $CDCl_3$) δ 8.38 (d, J = 8.0 Hz, 1H, H_{Ar}), 8.29 (d, J = 8.4 Hz, 1H, H_{Ar}), 8.13 (d, J = 8.4 Hz, 1H, H_{Ar}), 7.88 – 7.81 (m, 1H, H_{Ar}), 7.81 – 7.75 (m, 2H, H_{Ar}), 7.72 (ddd, J = 8.3, 6.9, 1.3 Hz, 1H, H_{Ar}), 7.52 (s, 1H, H_{Ar}), 7.51 – 7.43 (m, 1H, H_{Ar}), 7.37 (d, J = 7.6 Hz, 2H, H_{Ar}), 7.33 – 7.27 (m, 1H, H_{Ar}), 7.24 – 7.16 (m, 1H, H_{Ar}), 3.85 (s, 3H, NCH_3), 2.83 (s, 3H, CH_3); ^{13}C NMR (101 MHz, $CDCl_3$) δ 158.7, 156.5, 155.3, 148.8, 147.3, 147.2, 137.1, 136.8, 129.6, 129.4, 129.0, 126.2, 125.9, 124.8, 122.4, 121.7, 120.9, 119.1, 115.7, 109.7, 106.8, 94.4, 33.2, 25.5. IR (ν_{max}/cm^{-1}) 2923, 2360, 1584, 1561, 1541, 1477, 1451, 1226, 1101, 986; HRMS (ESI+) for $C_{24}H_{20}N_3$ $[M + H]^+$: calcd 350.1657, found 350.1653; LCMS 100% 13,2 min.

*4.2.6. General procedure for N functionalization of indole by CH_2OH (Method E): **31** and **37***

In a round bottom flask 1 equivalent of corresponding indole (0.09 mmol) was dissolved in EtOH (1 mL) and 0.5 mL of 10% NaOH aqueous solution and then 1 mL of HCOH 37% solution was added at room temperature for 5h. The solid was filtered with distilled water to give the product as a solid.

*4.2.6.1. (3-(3-(2-Methylquinolin-4-yl)phenyl)-1H-indol-1-yl)methanol **31***

31 was prepared according to the general method E from (**27**) (0.09 mmol). The filtration afforded 23 mg of the desired compound as a yellow powder (0.063 mmol, yield 70%). TLC (SiO_2, 5/5 cyclohexane/ EtOAc) R_f = 0.82; m.p. = 208-210 °C; ^{1}H NMR (400 MHz, DMSO-d_6) δ 8.03 (dd, J = 8.5, 1.2 Hz, 1H, H_{Ar}), 7.94 (d, J = 8.4 Hz, 1H, H_{Ar}), 7.91 (d, J = 7.5 Hz, 1H, H_{Ar}), 7.87 (s, 1H, H_{Ar}), 7.86 – 7.84 (m, 1H, H_{Ar}), 7.81 (t, J = 1.8 Hz, 1H, H_{Ar}), 7.74 (ddd, J = 8.4, 6.8, 1.5 Hz, 1H, H_{Ar}), 7.68 – 7.61 (m, 2H, H_{Ar}), 7.53 (ddd, J = 8.3, 6.8, 1.3 Hz, 1H, H_{Ar}), 7.47 (s, 1H, H_{Ar}), 7.42 (dt, J = 7.6, 1.4 Hz, 1H, H_{Ar}), 7.24 (ddd, J = 8.2, 7.0, 1.2 Hz, 1H, H_{Ar}), 7.15 (ddd, J = 8.1, 7.0, 1.1 Hz, 1H, H_{Ar}), 6.52 (t, J = 6.9 Hz, 1H, OH), 5.59 (d, J = 6.6 Hz, 2H, CH_2), 2.72 (s, 3H, CH_3); ^{13}C NMR (101 MHz, DMSO-d_6) δ 159.1, 148.5, 148.2, 138.65, 137.0, 136.4, 129.9, 129.9, 129.5, 128.0, 127.6, 127.2, 127.1, 126.6, 126.5, 125.8, 125.0, 122.8, 122.4, 121.0, 119.8, 115.7, 111.6, 69.5, 25.4; IR (ν_{max}/cm^{-1}) 2917, 2849, 2359, 1597, 1460, 1386, 1190, 1154, 1078, 1037, 771, 738,707; HRMS (ESI+) for $C_{25}H_{21}N_2O$ $[M + H]^+$: calcd 365.1654, found 365.1652; LCMS 100% 12,0 min.

*4.2.6.2. (3-(6-(3,4,5-Trimethoxyphenyl)pyridin-2-yl)-1H-indol-1-yl)methanol **37***

37 was prepared according to the general method E from (**35**) (0.09 mmol). The filtration afforded 20 mg of the desired compound as a white powder (0,051 mmol, yield 56%). TLC (SiO_2, 6/4 cyclohexane/EtOAc) R_f = 0.79; m.p. = 190 – 193 °C; ^{1}H NMR (300 MHz, acetone-d_6) δ 8.81 (dd, J = 6.4, 3.0 Hz, 1H, H_{Ar}), 8.14 (s, 1H, H_{Ar}), 7.85 – 7.68 (m, 3H, H_{Ar}), 7.65 (d, J = 2.3 Hz, 1H, H_{Ar}), 7.62 (s, 2H, H_{Ar}), 7.25 (ddt, J = 6.5, 4.7, 2.4 Hz, 2H, H_{Ar}), 5.77 (d, J = 7.0 Hz, 2H, CH_2), 5.57 (t, J = 7.4 Hz, 1H, OH), 3.99 (s, 6H, 2 OCH_3), 3.82 (s, 3H, OCH_3); ^{13}C NMR (75 MHz, acetone-d_6) δ 167.1, 166.8, 156.1, 154.8, 148.7, 148.2, 143.0, 138.1, 136.3, 129.3, 123.4, 123.2, 121.6, 118.8, 116.9, 111.4, 106.5, 105.3 (2C), 70.6, 60.8, 56.7 (2C); IR (ν_{max}/cm^{-1}) 3389, 3002, 2939, 1584, 1539, 1506, 1457, 1422, 1336, 1191, 1122, 1039, 999, 805, 749; HRMS (ESI+) for $C_{23}H_{23}N_2O_4$ $[M + H]^+$: calcd 391.1658, found 391.1663; LCMS 100% 17,5 min.

4.3. Biology

4.3.1. Cell culture and proliferation assay

Cancer cell lines were obtained from the American Type Culture Collection (Rockville, MD, USA) and were cultured according to the supplier's instructions. K562R (doxorubicin-resistant) leukemia cells were a generous gift from JP Marie (France). Human HCT-116 colorectal carcinoma cells were grown in Gibco McCoy's 5A supplemented with 10% fetal calf serum (FCS) and 1% glutamine. A549 lung carcinoma, K562 and K562R leukemia cells were grown in RPMI 1640 supplemented with 10% fetal calf serum and 1% glutamine. MCF7 breast adenocarcinoma, HT29 colon carcinoma and Mia-Paca2 pancreatic carcinoma cells were grown in Gibco medium DMEM supplemented with 10% fetal calf serum (FCS) and 1% glutamine. Human HeLa cells were obtained from the American Type Culture Collection and cultured at 37 °C in 5% CO_2 in the recommended media supplemented with 10% fetal bovine serum (51810-500, Dutscher). Cell lines were maintained at 37 °C in a humidified atmosphere containing 5% CO_2. Cell viability was determined by a luminescent assay according to the manufacturer's instructions (Promega, Madison, WI, USA). For IC_{50} determination, the cells were seeded in 96-well plates (3 × 103 cells/well) containing 100 µL of growth medium. After 24 h of culture, the cells were treated with the tested compounds at 10 different final concentrations. Each concentration was obtained from serial dilutions in culture medium starting from the stock solution. Control cells were treated with the vehicle. All the compounds were solubilized in DMSO and diluted in culture medium to obtain a final concentration of 0.1 % of DMSO in cell culture. Experiments were performed in triplicate. After 72 h of incubation, 100 µL of Cell Titer Glo Reagent was added for 15 min before recording luminescence with a spectrophotometric plate reader PolarStar Omega (BMG LabTech). The dose-response curves were plotted with Graph Prism software and the IC_{50} values were calculated using the Graph Prism software from polynomial curves (four or five-parameter logistic equations).

Cell cycle analysis. After 24h of treatment with **42**, K562 cells were fixed in 70% ethanol and stained with propidium iodide solution containing RNase A. DNA content was further determined by flow cytometry using FC500 (Beckman Coulter).

4.3.2. Cell-based assay for the quantification of the effect of drugs on microtubules

This procedure was adapted from Ramirez-Rios et al.[41] 7,500 HeLa cells were seeded in 96-well microplates (Greiner #655083) in 100 µL of complete medium per well and then incubated at 37 °C in 5% CO_2. 24 hours after seeding, cells were treated with compounds (1 concentration per column, 1 plate per molecule) at different concentrations or DMSO at 0.1%, which was used as a positive control. At the end of the incubation, the medium was aspirate. Cells were permeabilized for 10 minutes at 37 °C using 100 µL per well of OPT buffer (80 mM Pipes, 1 mM EGTA, 1 mM $MgCl_2$, 0.5% Triton X-100, and 10% glycerol, pH 6.8) pre-warmed to 37 °C. After buffer aspiration, cells were fixed overnight at room temperature using 100 µL per well of 4% formaldehyde in PBS pH 7.2. Cells were washed 3 times in PBS pH 7.2, 0.1% Tween-20 (150 µL per well). Then 50 µl of α3A1 anti-tubulin antibody (1/5,000 in PBS pH 7.4, 0.3% BSA, 0.03% NaN_3) were added for 45 minutes. After washing of cells as described above, 50 µl of anti-mouse antibody coupled to HRP (1/2,000 in PBS pH 7.4, 0.3% BSA, 0.03% NaN_3) were added for 45 minutes. Then cells were washed again. The microplate was placed into the BMG FLUOstar OPTIMA Microplate Reader and 100 µl of ECL Western blotting substrate (Biorad Clarity) were injected to each well. The luminescent signal was read immediately after injection.

4.3.3. Immunofluorescence

Cells were fixed and processed for immunofluorescence analysis of the MT network as previously described,[46] using anti-α-tubulin clone α3A1,[47] as primary antibody and a secondary antibody coupled to Alexa 488 (Jackson Immuno-Research Laboratories, 115-545-003). DNA was stained with 20 μM Hoechst 33342 (Sigma, #23491-52-3). Images were captured with a Zeiss AxioimagerM2 microscope equipped with the acquisition software AxioVision.

4.3.3. In vitro microtubule assembly assay

Pure tubulin (purchased at the Centro de Investigaciones Biológicas, CSIC, Madrid, Spain) was equilibrated in 100 mM MES, 1 mM EGTA, 1 mM $MgCl_2$, pH 6.8 buffer and centrifuged at 75,000 rpm for 10 minutes in an TLA-100 rotor in a Beckman Optima TLX centrifuge. Tubulin was then diluted to 50 μM. The samples were supplemented with the desired drug (or the vehicle, i.e. DMSO) and incubated for 30 min at 4 °C. Microplates ((half area, 96 well- microplates, Greiner ref 675096)) were then transferred to a thermostatically controlled reader (37 °C, BMG FLUOstar OPTIMA). Assembly kinetics was initiated by addition of GTP 1 mM and followed by measuring the absorbance of the samples at 350 nm.

4.3.4. Mitochondrial membrane potential Assay

One of the hallmarks for apoptosis is the loss of mitochondrial membrane potential (ΔΨm). The changes in the mitochondrial potential were detected by 5,5',6,6'-tetrachloro-1,1',3,3' tetraethylbenzimidazolylcarbocya-nine iodide/chloride (JC-1), a cationic dye that exhibits potential dependent accumulation in mitochondria, indicated by fluorescence emission shift from red (590 nm) to green (525 nm). In brief, K562 cells were treated with different concentrations of compound **42** for 24h. After treatment, cells were re-suspended in 1 ml of PBS containing 2 μM final concentration JC-1 probe and incubated at 37 °C for 15 min. Analysis of cells was performed on a FC500 flow cytometer (Beckman Coulter, France).

4.3.5. Cytotoxicity Evaluations in Peripheral Blood Lymphocytes (PBL)

The cytotoxicity of compound **42** was compared to that of isoCA-4 in quiescent and proliferating peripheral blood lymphocytes (PBLs). Peripheral blood mononuclear cells were obtained from one healthy donor by density gradient centrifugation using Ficoll-Paque PREMIUM (GE Healthcare) and cultured overnight at 37 °C in RPMI-1640 medium containing 10% fetal calf serum (complete RPMI-1640 medium). Non-adherent cells were harvested, and diluted at $1.11x10^5$/mL in complete RPMI-1640 medium containing or not phytohemagglutinin (PHA, final concentration 2.5 μg/mL), which is a potent mitogen inducing activation and proliferation of lymphocytes. Untreated (quiescent) and PHA-treated (proliferating) PBLs (90 μL, 10.000 cells/well) were plated in white walled 96-well plates and cultured overnight at 37 °C.

Quiescent and proliferating PBLs were then treated in triplicate with various concentrations of *iso*CA-4 and compound **42** (final concentrations: $2.5x10^{-5}$ M, $1x10^{-5}$ M, $2.5x10^{-6}$ M, $1x10^{-6}$ M, $2.5x10^{-7}$ M, $1x10^{-7}$ M, $2.5x10^{-8}$ M, $1x10^{-8}$ M, $2.5x10^{-9}$ M, $1x10^{-9}$ M, $2.5x10^{-10}$ M, $1x10^{-10}$ M, $2.5x10^{-11}$ M and $1x10^{-11}$ M) for 72 h at 37 °C. To this purpose, stock solutions of isoCA-4 and **42** were prepared by dissolving them in DMSO at a concentration of 10 mM, and both compounds were serially diluted in DMSO. Ten μL of each dilution or DMSO were diluted 1:100 in complete RPMI-1640 medium, and 10 μL of these dilutions were then added to quiescent and proliferating PBLs (90 μL). The final concentration of DMSO was 0.25% for each well. After 72 h of incubation, cell viability was determined by adding 100 μL of CellTiter Glo Reagent, as previously described for cancer cell lines.

Luminescence was recorded on a FLUOstar Omega (BMG LabTech), and IC_{50} values were calculated from the corresponding dose-response curves using the Graph Pad Prism software.

5. Molecular docking

Atomic coordinates for tubulin α,β-dimer were retrieved from the Protein Data Bank (accession code 6H9B).[27] Missing hydrogen atoms were added using the Dock Prep module from the UCSF Chimera v1.13 software package,[48] and atoms from the ligand co-crystallized in the colchicine binding at the interface between chains C and D were deleted. Coordinates for a low-energy starting conformer of compound **42** were obtained using the Conformers function from MarvinSketch v19.12 software package[49] with default parameters. Molecular docking was performed using AutoDock Vina v1.1.2 software package[50] with default parameters and the binding site defined as the box circumscribed to all the protein residues in contact with the co-crystallized ligand. Analysis and depiction of poses were performed using UCSF Chimera v1.13 software package.[48]

Acknowledgments

The authors acknowledge support of this project by the CNRS and University Paris-Saclay. S. Pecnard thanks La Ligue Contre le Cancer for the financing of his Ph.D. Our laboratory is a member of the Laboratory of Excellence LERMIT supported by a grant (ANR-10-LABX-33).

References

[1] J. Roostalu, T. Surrey, Microtubule nucleation: beyond the template, Nat. Rev. Mol. Cell. Biol., 18 (2017) 702-710.
[2] G.J. Brouhard, L.M. Rice, Microtubule dynamics: an interplay of biochemistry and mechanics, Nat. Rev. Mol. Cell. Biol. , 19 (2018) 451-463.
[3] M.A. Jordan, L. Wilson, Microtubules as a target for anticancer drugs, Nat. Rev. Cancer, 4 (2004) 253-265.
[4] R. Kaur, G. Kaur, R.K. Gill, R. Soni, J. Bariwal, Recent developments in tubulin polymerization inhibitors: An overview, Eur. J. Med. Chem., 87 (2014) 89-124.
[5] C. Dumontet, M.A. Jordan, Microtubule-binding agents: a dynamic field of cancer therapeutics, Nat. Rev. Drug Discov., 9 (2010) 790-803.
[6] S.A. Hill, S.J. Lonergan, J. Denekamp, D.J. Chaplin, Vinca alkaloids: Anti-vascular effects in a murine tumour, Eur. J. Cancer, 29 (1993) 1320-1324.
[7] G.R. Pettit, S.B. Singh, E. Hamel, C.M. Lin, D.S. Alberts, D. Garcia-Kendal, Isolation and structure of the strong cell growth and tubulin inhibitor combretastatin A-4, Experientia, 45 (1989) 209-211.
[8] A. Hamze, M. Alami, O. Provot, Developments of isoCombretastatin A-4 derivatives as highly cytotoxic agents, Eur. J. Med. Chem., 190 (2020) 112110.
[9] Z.S. Seddigi, M.S. Malik, A.P. Saraswati, S.A. Ahmed, A.O. Babalghith, H.A. Lamfon, A. Kamal, Recent advances in combretastatin based derivatives and prodrugs as antimitotic agents, Medchemcomm, 8 (2017) 1592-1603.
[10] C.M. Lin, H.H. Ho, G.R. Pettit, E. Hamel, Antimitotic natural products combretastatin A-4 and combretastatin A-2: studies on the mechanism of their inhibition of the binding of colchicine to tubulin, Biochemistry, 28 (1989) 6984-6991.
[11] G.G. Dark, S.A. Hill, V.E. Prise, G.M. Tozer, G.R. Pettit, D.J. Chaplin, Combretastatin A-4, an Agent That Displays Potent and Selective Toxicity toward Tumor Vasculature, Cancer Res., 57 (1997) 1829-1834.

[12] R. Grisham, B. Ky, K.S. Tewari, D.J. Chaplin, J. Walker, Clinical trial experience with CA4P anticancer therapy: focus on efficacy, cardiovascular adverse events, and hypertension management, Gynaecol. Oncol. Res. Pract., 5 (2018) 1.
[13] D.W. Siemann, D.J. Chaplin, M.R. Horsman, Realizing the Potential of Vascular Targeted Therapy: The Rationale for Combining Vascular Disrupting Agents and Anti-Angiogenic Agents to Treat Cancer, Cancer Invest., 35 (2017) 519-534.
[14] R. Gaspari, A.E. Prota, K. Bargsten, A. Cavalli, M.O. Steinmetz, Structural Basis of *cis*- and *trans*-Combretastatin Binding to Tubulin, Chem, 2 (2017) 102-113.
[15] S. Aprile, E. Del Grosso, G.C. Tron, G. Grosa, In Vitro Metabolism Study of Combretastatin A-4 in Rat and Human Liver Microsomes, Drug Metab. Dispos., 35 (2007) 2252-2261.
[16] For reviews, see. Y. Lu, J. Chen, M. Xiao, W. Li, D.D. Miller, An Overview of Tubulin Inhibitors That Interact with the Colchicine Binding Site, Pharm. Res. , 29 (2012) 2943-2971.
[17] A. Hamze, A. Giraud, S. Messaoudi, O. Provot, J.-F. Peyrat, J. Bignon, J.-M. Liu, J. Wdzieczak-Bakala, S. Thoret, J. Dubois, J.-D. Brion, M. Alami, Synthesis, biological evaluation of 1,1-diarylethylenes as a novel class of antimitotic agents, ChemMedChem, 4 (2009) 1912-1924.
[18] S. Messaoudi, B. Treguier, A. Hamze, O. Provot, J.-F. Peyrat, J.R. De Losada, J.-M. Liu, J. Bignon, J. Wdzieczak-Bakala, S. Thoret, J. Dubois, J.-D. Brion, M. Alami, Isocombretastatins A versus Combretastatins A: The Forgotten isoCA-4 Isomer as a Highly Promising Cytotoxic and Antitubulin Agent, J. Med. Chem., 52 (2009) 4538-4542.
[19] A. Hamze, E. Rasolofonjatovo, O. Provot, C. Mousset, D. Veau, J. Rodrigo, J. Bignon, J.M. Liu, J. Wdzieczak-Bakala, S. Thoret, J. Dubois, J.D. Brion, M. Alami, B-Ring-modified isoCombretastatin A-4 analogues endowed with interesting anticancer activities, ChemMedChem, 6 (2011) 2179-2191.
[20] M. Lawson, A. Hamze, J.F. Peyrat, J. Bignon, J. Dubois, J.D. Brion, M. Alami, An efficient coupling of *N*-tosylhydrazones with 2-halopyridines: Synthesis of 2-alpha-styrylpyridines endowed with antitumor activity, Org. Biomol. Chem., 11 (2013) 3664-3673.
[21] A. Maksimenko, M. Alami, F. Zouhiri, J.D. Brion, A. Pruvost, J. Mougin, A. Hamze, T. Boissenot, O. Provot, D. Desmaele, P. Couvreur, Therapeutic modalities of squalenoyl nanocomposites in colon cancer: An ongoing search for improved efficacy, Acs Nano, 8 (2014) 2018-2032.
[22] A. Hamze, How do we improve histone deacetylase inhibitor drug discovery?, Expert Opin. Drug Discov., 15 (2020) 527-529.
[23] I. Khelifi, T. Naret, D. Renko, A. Hamze, G. Bernadat, J. Bignon, C. Lenoir, J. Dubois, J.-D. Brion, O. Provot, M. Alami, Design, synthesis and anticancer properties of IsoCombretaQuinolines as potent tubulin assembly inhibitors, Eur. J. Med. Chem., 127 (2017) 1025-1034.
[24] M.A. Soussi, O. Provot, G. Bernadat, J. Bignon, D. Desravines, J. Dubois, J.-D. Brion, S. Messaoudi, M. Alami, IsoCombretaQuinazolines: Potent Cytotoxic Agents with Antitubulin Activity, ChemMedChem, 10 (2015) 1392-1402.
[25] S. Zheng, Q. Zhong, M. Mottamal, Q. Zhang, C. Zhang, E. LeMelle, H. McFerrin, G. Wang, Design, Synthesis, and Biological Evaluation of Novel Pyridine-Bridged Analogues of Combretastatin-A4 as Anticancer Agents, J. Med. Chem., 57 (2014) 3369-3381.
[26] T. Bzeih, T. Naret, A. Hachem, N. Jaber, A. Khalaf, J. Bignon, J.-D. Brion, M. Alami, A. Hamze, A general synthesis of arylindoles and (1-arylvinyl)carbazoles via a one-pot reaction from *N*-tosylhydrazones and 2-nitro-haloarenes and their potential application to colon cancer, Chem. Commun., 52 (2016) 13027-13030.
[27] T. Naret, I. Khelifi, O. Provot, J. Bignon, H. Levaique, J. Dubois, M. Souce, A. Kasselouri, A. Deroussent, A. Paci, P.F. Varela, B. Gigant, M. Alami, A. Hamze, 1,1-Diheterocyclic Ethylenes Derived from Quinaldine and Carbazole as New Tubulin-Polymerization Inhibitors: Synthesis, Metabolism, and Biological Evaluation, J. Med. Chem., 62 (2019) 1902-1916.
[28] I. Khelifi, T. Naret, A. Hamze, J. Bignon, H. Levaique, M.C. Garcia Alvarez, J. Dubois, O. Provot, M. Alami, N,N-bis-heteroaryl methylamines: Potent anti-mitotic and highly cytotoxic agents, Eur. J. Med. Chem., 168 (2019) 176-188.
[29] T. Bzeih, D. Lamaa, G. Frison, A. Hachem, N. Jaber, J. Bignon, P. Retailleau, M. Alami, A. Hamze, Csp2-Csp2 and Csp2-N Bond Formation in a One-Pot Reaction between N-Tosylhydrazones and

Bromonitrobenzenes: An Unexpected Cyclization to Substituted Indole Derivatives, Org. Lett., 19 (2017) 6700-6703.
[30] T. Bzeih, K. Zhang, A. Khalaf, A. Hachem, M. Alami, A. Hamze, One-Pot Reaction between N-Tosylhydrazones and 2-Nitrobenzyl Bromide: Route to NH-Free C2-Arylindoles, J. Org. Chem., 84 (2019) 228-238.
[31] For review on Cadogan reaction, see M. Kaur, R. Kumar, C-N and N-N bond formation via Reductive Cyclization: Progress in Cadogan /Cadogan-Sundberg Reaction‡, ChemistrySelect, 3 (2018) 5330-5340.
[32] T. Naret, T. Bzeih, P. Retailleau, M. Alami, A. Hamze, One-Pot Selective Functionalization of Nitrogen-Containing Heterocycles with N-tosylhydrazones and Amines, Adv. Synth. Catal., 360 (2018) 584-594.
[33] K. Zhang, A. El Bouakher, H. Levaique, J. Bignon, P. Retailleau, M. Alami, A. Hamze, Pyrrolo-imidazo[1,2-a]pyridine Scaffolds through a Sequential Coupling of N-Tosylhydrazones with Imidazopyridines and Reductive Cadogan Annulation, Synthetic Scope, and Application, J. Org. Chem., 84 (2019) 13807-13823.
[34] K. Zhang, A. El Bouakher, H. Lévaique, J. Bignon, P. Retailleau, M. Alami, A. Hamze, Imidazodipyridines via DMAP Catalyzed Domino N−H Carbonylation and 6π-Electrocyclization: Synthetic Scope and Application, Adv. Synth. Catal., 362 (2020) 3243-3256.
[35] D. Simoni, G. Grisolia, G. Giannini, M. Roberti, R. Rondanin, L. Piccagli, R. Baruchello, M. Rossi, R. Romagnoli, F.P. Invidiata, S. Grimaudo, M.K. Jung, E. Hamel, N. Gebbia, L. Crosta, V. Abbadessa, A. Di Cristina, L. Dusonchet, M. Meli, M. Tolomeo, Heterocyclic and Phenyl Double-Bond-Locked Combretastatin Analogues Possessing Potent Apoptosis-Inducing Activity in HL60 and in MDR Cell Lines, J. Med. Chem., 48 (2005) 723-736.
[36] A. Giraud, O. Provot, A. Hamzé, J.-D. Brion, M. Alami, One-pot hydrosilylation–protodesilylation of functionalized diarylalkynes: a highly selective access to Z-stilbenes. Application to the synthesis of combretastatin A-4, Tetrahedron Letters, 49 (2008) 1107-1110.
[37] D. Lamaa, E. Messe, V. Gandon, M. Alami, A. Hamze, Toward a Greener Barluenga-Valdes Cross-Coupling: Microwave-Promoted C-C Bond Formation with a Pd/PEG/H2O Recyclable Catalytic System, Org. Lett., 21 (2019) 8708-8712.
[38] D. Lamaa, H.P. Lin, L. Zig, C. Bauvais, G. Bollot, J. Bignon, H. Levaique, O. Pamlard, J. Dubois, M. Ouaissi, M. Souce, A. Kasselouri, F. Saller, D. Borgel, C. Jayat-Vignoles, H. Al-Mouhammad, J. Feuillard, K. Benihoud, M. Alami, A. Hamze, Design and Synthesis of Tubulin and Histone Deacetylase Inhibitor Based on iso-Combretastatin A-4, J. Med. Chem., 61 (2018) 6574-6591.
[39] R. Schobert, K. Effenberger-Neidnicht, B. Biersack, Stable combretastatin A-4 analogues with sub-nanomolar efficacy against chemoresistant HT-29 cells, Int. J. Clin. Pharmacol. Ther., 49 (2011) 71-72.
[40] J. Cummings, N. Zelcer, J.D. Allen, D. Yao, G. Boyd, M. Maliepaard, T.H. Friedberg, J.F. Smyth, D.I. Jodrell, Glucuronidation as a mechanism of intrinsic drug resistance in colon cancer cells: contribution of drug transport proteins, Biochem. Pharmacol., 67 (2004) 31-39.
[41] S. Ramirez-Rios, S. Michallet, L. Peris, C. Barette, C. Rabat, Y. Feng, M.-O. Fauvarque, A. Andrieux, K. Sadoul, L. Lafanechère, A New Quantitative Cell-Based Assay Reveals Unexpected Microtubule Stabilizing Activity of Certain Kinase Inhibitors, Clinically Approved or in the Process of Approval, Front. Pharmacol., 11, 543, 10.3389/fphar.2020.00543(2020).
[42] J.C. Lee, S.N. Timasheff, In vitro reconstitution of calf brain microtubules: effects of solution variables, Biochemistry, 16 (1977) 1754-1764.
[43] H. Vakifahmetoglu-Norberg, A.T. Ouchida, E. Norberg, The role of mitochondria in metabolism and cell death, Biochem. Biophys. Res. Commun., 482 (2017) 426-431.
[44] J.B. Spinelli, M.C. Haigis, The multifaceted contributions of mitochondria to cellular metabolism, Nat. Cell Biol. , 20 (2018) 745-754.
[45] T. Naret, I. Khelifi, O. Provot, J. Bignon, H. Levaique, J. Dubois, M. Souce, A. Kasselouri, A. Deroussent, A. Paci, P.F. Varela, B. Gigant, M. Alami, A. Hamze, 1,1-Diheterocyclic Ethylenes Derived

from Quinaldine and Carbazole as New Tubulin-Polymerization Inhibitors: Synthesis, Metabolism, and Biological Evaluation, J. Med. Chem., 62 (2019) 1902-1916.
[46] R. Prudent, E. Vassal-Stermann, C.-H. Nguyen, C. Pillet, A. Martinez, C. Prunier, C. Barette, E. Soleilhac, O. Filhol, A. Beghin, G. Valdameri, S. Honoré, S. Aci-Sèche, D. Grierson, J. Antonipillai, R. Li, A. Di Pietro, C. Dumontet, D. Braguer, J.-C. Florent, S. Knapp, O. Bernard, L. Lafanechère, Pharmacological Inhibition of LIM Kinase Stabilizes Microtubules and Inhibits Neoplastic Growth, Cancer Res., 72 (2012) 4429-4439.
[47] L. Peris, M. Thery, J. Fauré, Y. Saoudi, L. Lafanechère, J.K. Chilton, P. Gordon-Weeks, N. Galjart, M. Bornens, L. Wordeman, J. Wehland, A. Andrieux, D. Job, Tubulin tyrosination is a major factor affecting the recruitment of CAP-Gly proteins at microtubule plus ends, J. Cell Biol., 174 (2006) 839-849.
[48] E.F. Pettersen, T.D. Goddard, C.C. Huang, G.S. Couch, D.M. Greenblatt, E.C. Meng, T.E. Ferrin, UCSF Chimera—A visualization system for exploratory research and analysis, J. Comput. Chem., 25 (2004) 1605-1612.
[49] http://www.chemaxon.com
[50] O. Trott, A.J. Olson, AutoDock Vina: Improving the speed and accuracy of docking with a new scoring function, efficient optimization, and multithreading, J. Comput. Chem., 31 (2010) 455-461.

Table 1. Effect of designed compounds on HCT116 cell viability.[a]

	compd	HCT116 (nM)[b]		compd	HCT116 (nM)[b]
16	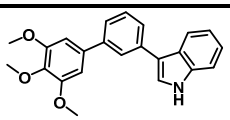	70 ± 15	**35**	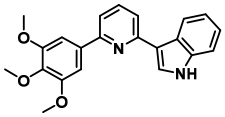	20 ± 1.9
17	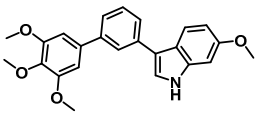	4910 ± 600	**36**	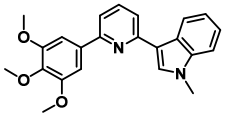	400 ± 150
18	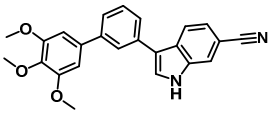	7630 ± 650	**37**	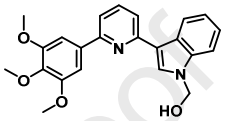	90.2 ± 1.7
19	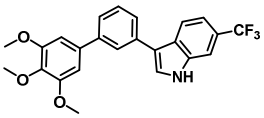	3220 ± 780	**42**	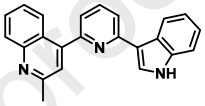	2.2 ± 0.4
20	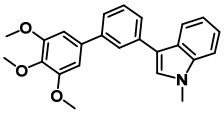	490 ± 120	**43**	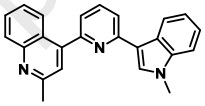	267 ± 26
28	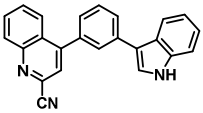	175 ± 21.2	**47**	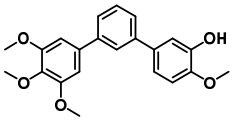	4564 ± 148
29	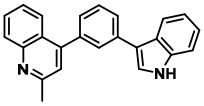	40 ± 1.4	**8**	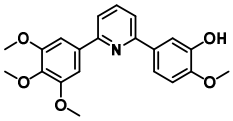	1300 ± 120
30	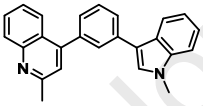	70 ± 4.2	**1** CA-4	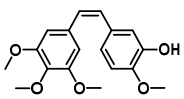	2.6 ± 0.6[c]
31	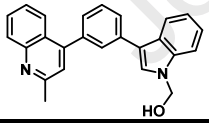	79 ± 19	**3** *iso*CA4	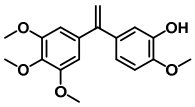	2.4 ± 0.9

[a] HCT-116 human colon carcinoma cells. [b] Compound concentration required to decrease cell growth by 50%; values represent the average SD of three experiments. [c] The IC_{50} value for CA-4[36] and *iso*CA-4[37, 38] were determined in this study.

Table 2. Effects on cell viability of compound **42** against a panel of seven human cancer cell lines, IC_{50} values are reported in nM.

Compd	**HCT116**[a]	**K562**[b]	**K562R**[c]	**MiaPaca2**[d]	**A549**[e]	**MCF7**[f]	**HT-29**[h]
Tumor Type	Colon	Leukemia	Leukemia	Pancreas	Lung	Breast	Colon
42	2.2 ± 0.4	4.5 ± 0.5	2.0 ± 0.9	3.6 ± 0.4	8.0 ± 0.25	10.1 ± 1.0	9.1 ± 0.38
***iso*CA4**	2.4 ± 0.9	5.2 ± 0.2	3.0 ± 0.2	10 ± 1.2	10 ± 0.1	8 ± 0.4	275 ± 22
CA-4	2.7 ± 0.3	5.5 ± 0.4	25 ± 0.05	8 ± 2	200 ± 5	170 ± 5	>8000

[a] Colon-carcinoma cells (HCT116); [b] Chronic myelogenous leukemia cells (K562); [c] Doxorubicin-resistant chronic myeloid leukemia cells (K562R); [d] Human pancreatic carcinoma (MiaPaca2); [e] Adenocarcinoma human alveolar basal epithelial cells (A549); [f] Breast cancer cell line (MCF-7); Human colon cancer cell line (HT-29).

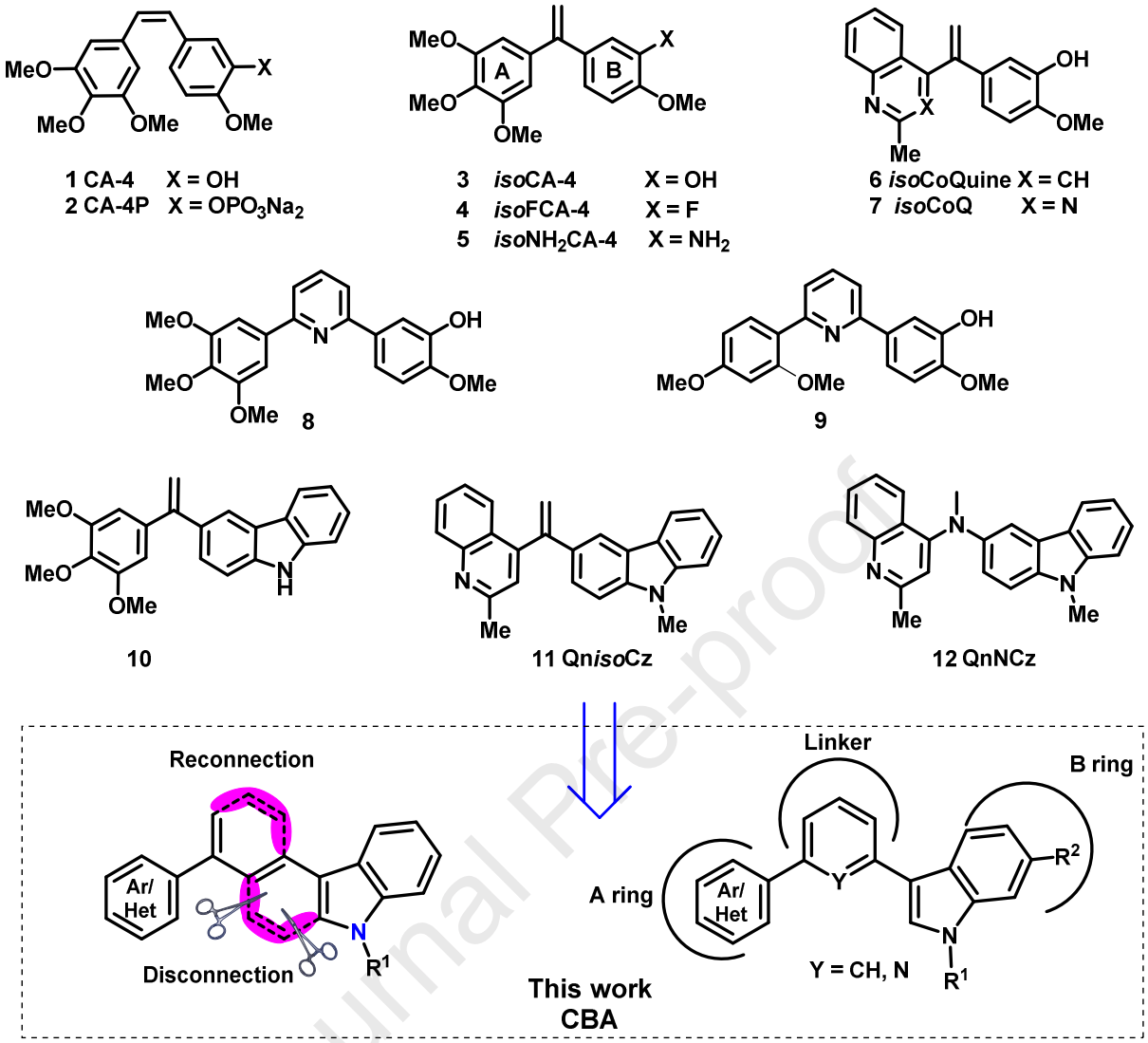

Fig. 1. Structures of CA-4, *iso*CA-4 derivatives, synthetic analogs and target **C**yclic **B**ridged **A**nalogs **CBA**

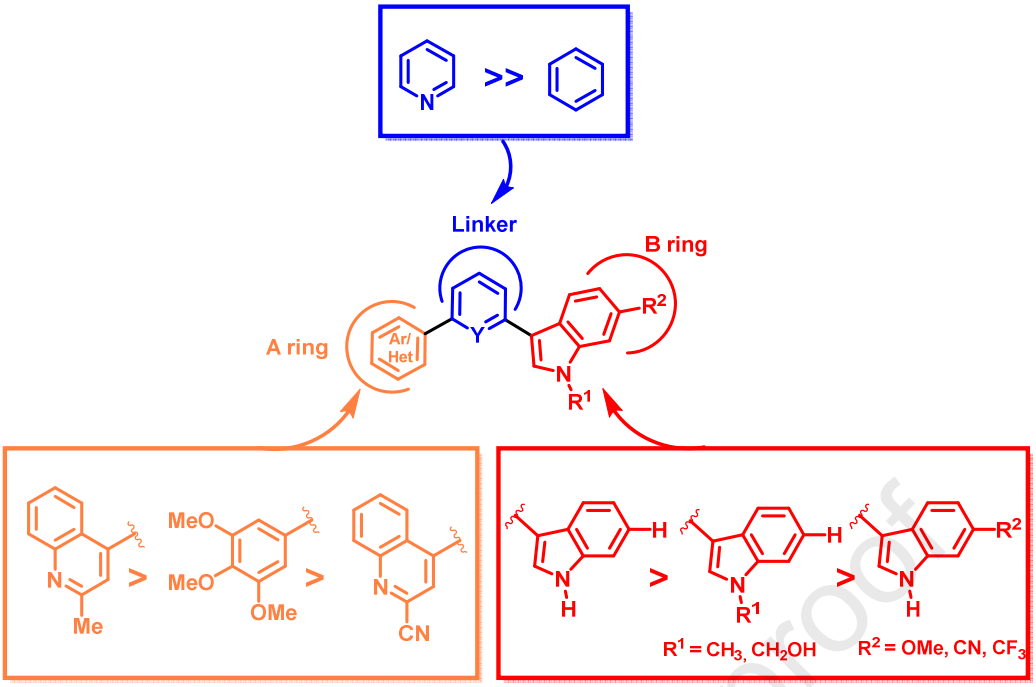

Fig. 2. Summary of the SARs study of target compounds based on cell viability evaluated on a human colon cancer cell line.

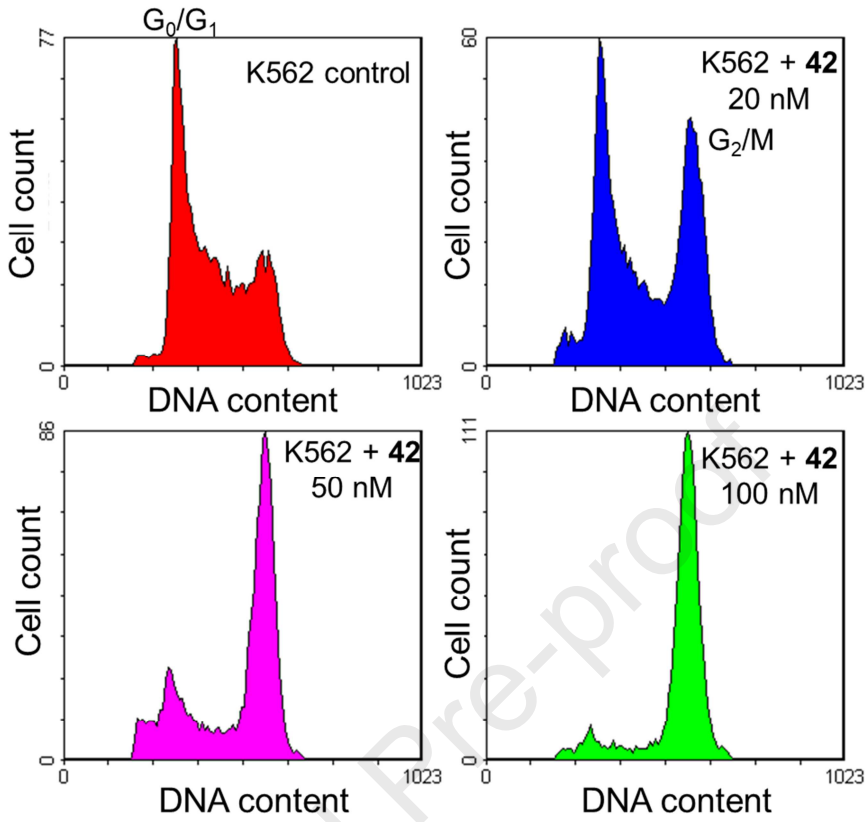

	G0/G1	S	G2/M
NT	22,8	60,2	17
20 nM	23,4	40,9	35,7
50 nM	19,8	22,6	57,6
100 nM	5,6	13,1	81,3

Fig. 3. Effect of compound **42** on the cell cycle of K562 cell lines. One representative replicate out of two is shown.

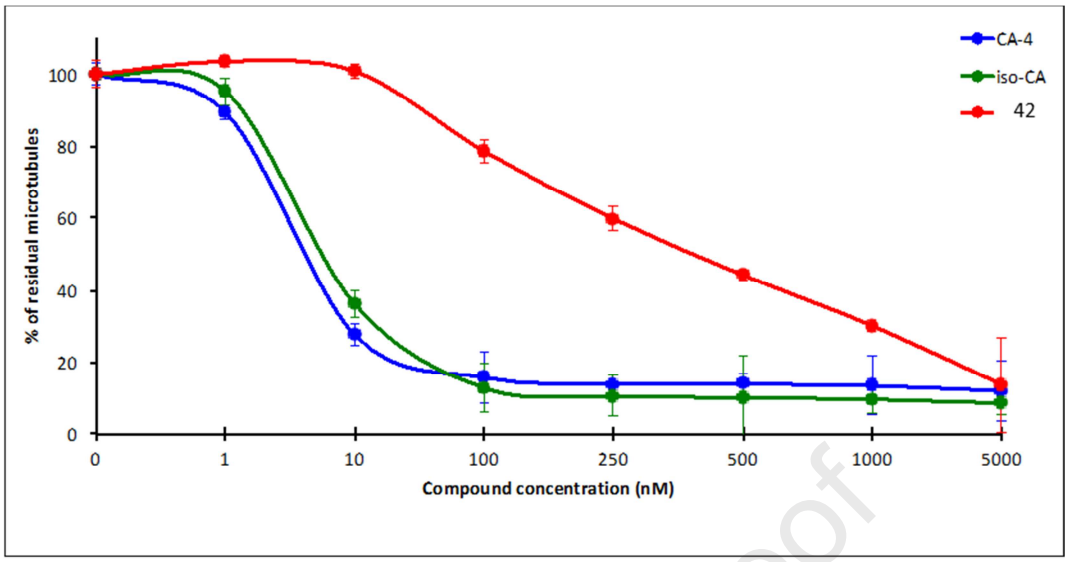

Fig. 4. Comparative analysis of the effect of 42, CA-4, and *iso*-CA4 on microtubule dynamics in HeLa cells. Different doses of the compounds were applied to HeLa cells in microplates and the amount of residual microtubules was assessed after 2 hours, using a luminescent assay described in the material and methods section. Results are expressed as mean ± SEM of their independent experiments.

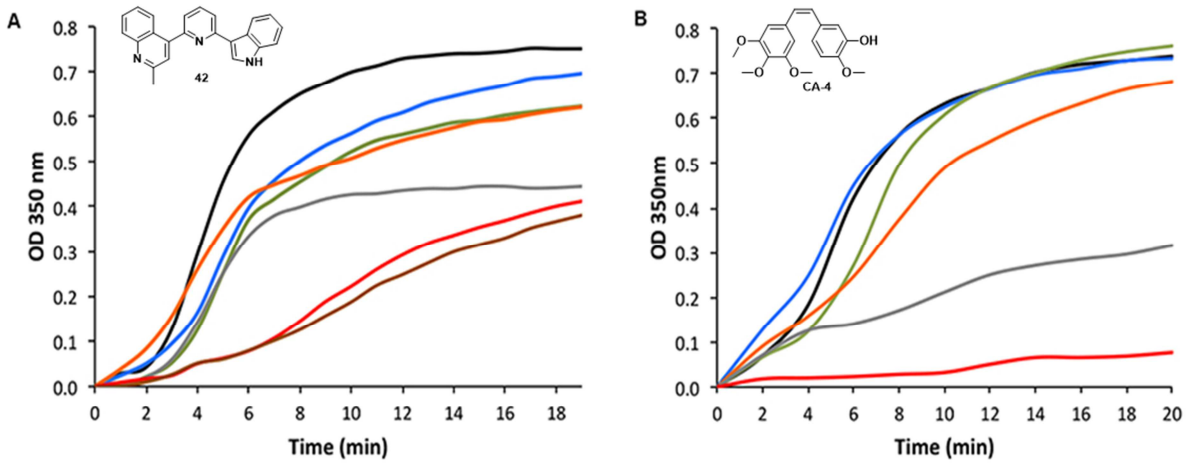

Fig. 5 Comparison of the effect of compound **42** and CA-4 on tubulin polymerization. Compound **42** (A) or CA-4 (B) were added at different concentrations to 50 µM tubulin and their effect on tubulin kinetics assembly was monitored. Black: DMSO (control); blue: 0.1 µM; green: 0.5 µM; orange: 1 µM; grey: 2.5 µM; red: 5 µM; brown: 7 µM. Representative curves of two independent experiments.

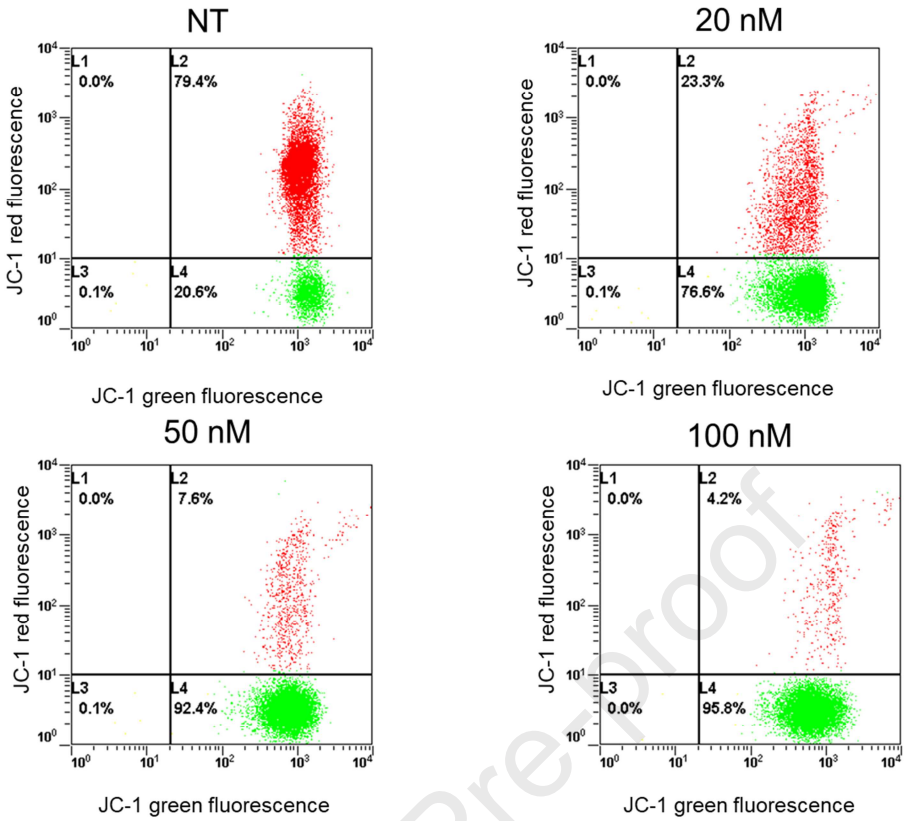

Fig. 6 Compound **42** induced mitochondrial dysfunctions in K562 leukemia cells. Cells were incubated with **42** at concentrations of 20, 50, 100 nM for 24 h at 37 °C. The portion of mitochondria dysfunction was measured using the JC1 assay.

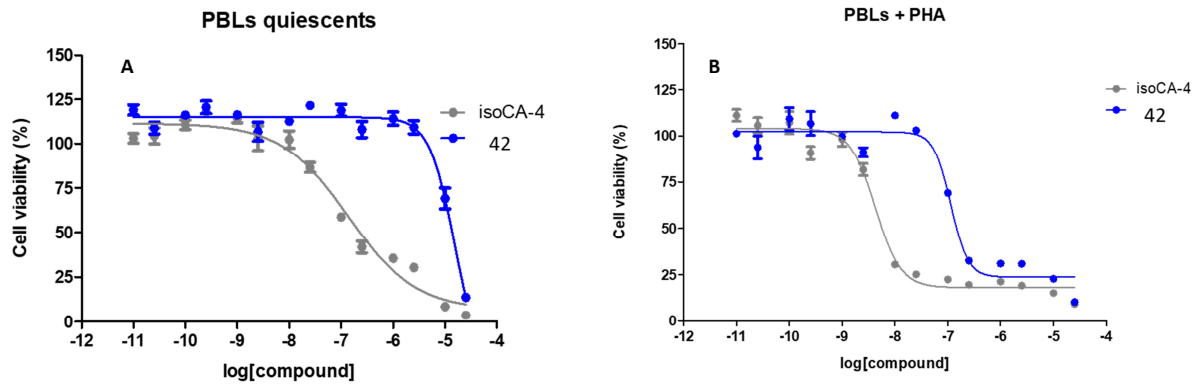

Fig. 7. Cytotoxicity of compound **42** and *iso*CA-4 in peripheral blood lymphocytes (PBLs). (A) Quiescent PBLs (10.000/well) from one healthy donor were treated in triplicate with various concentrations (10-11-2.5 x 10^{-5} M) of *iso*CA-4 and compound **42** for 72 h at 37 °C, and cell viability was measured by a luminescent assay. A cell viability of 100% corresponds to the mean luminescence value obtained for vehicle (0.25% DMSO)-treated PBLs, and data represent the mean (± standard error of the mean, SEM). Dose-response curves were fitted to a log(inhibitor) *vs* response curve using the Graph Pad Prism software, yielding IC_{50} values of 137 nM and >10 µM for *iso*CA-4 and compound **42**, respectively. Compounds could not be tested at higher concentrations than 25 µM, precluding more accurate determination of the IC_{50} value for compound **42**. (B) PBLs from the same donor (10.000/well) were activated with phytohemagglutinin (PHA. 2.5 µg/mL) to induce their proliferation, and were subsequently treated in triplicate with various concentrations (10-11-2.5 x 10^{-5} M) of *iso*CA-4 and compound **42** for 72 h at 37 °C. Cell viability was calculated as described for quiescent PBLs, and data represent the mean (± standard error of the mean, SEM). Dose-response curves were fitted to a log(inhibitor) vs response curve using the Graph Pad Prism software, yielding IC_{50} values of 4.3 nM and 114 nM for *iso*CA-4 and compound **42**, respectively

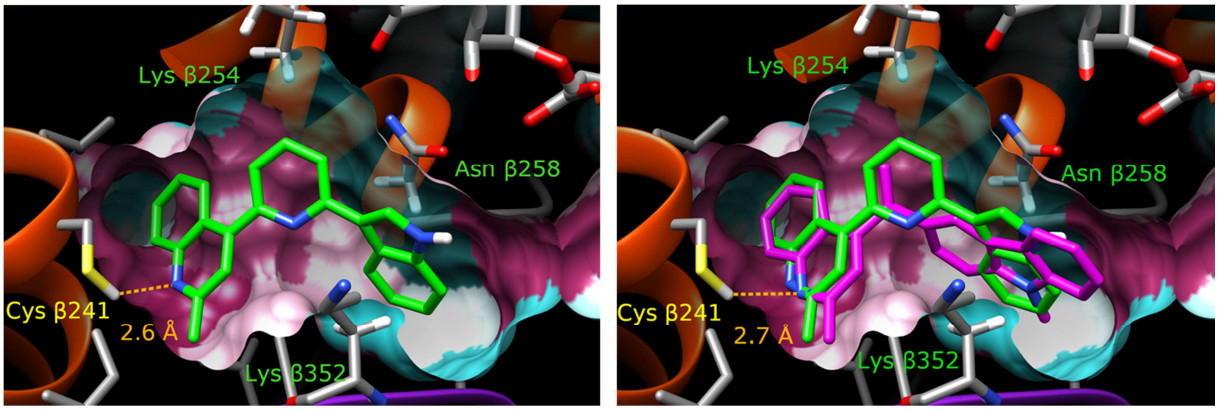

Fig. 8. (a) Putative binding mode of compound **42** (green color) within colchicine binding site of tubulin X-ray structure (accession code 6H9B). (b) same figure with previously reported binding mode of reference compound **11** in overlay (magenta color). Showing expected hydrogen bonds between nitrogen of quinoline moiety and cysteine β241, and plausible hydrophobic interactions.

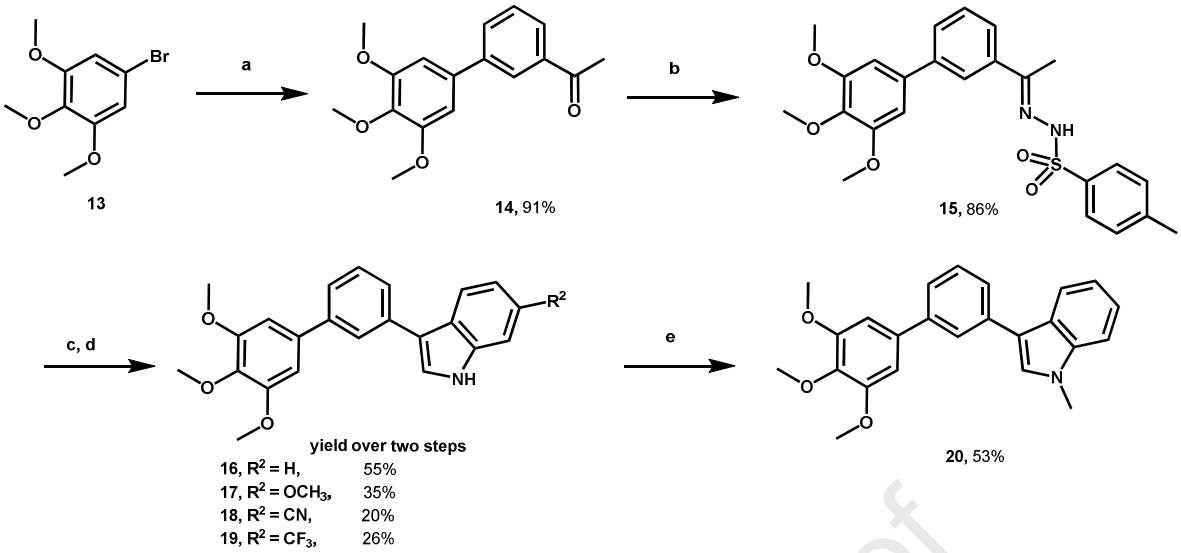

Scheme 1. Reagents and conditions: (a) 3-acetylphenyl-boronic acid, $Pd(OAc)_2$, SPhos, $K_3PO_4.H_2O$, cyclopentyl methyl ether (CPME)/H_2O, 110 °C; (b) 4-methylbenzenesulfonohydrazide, EtOH, reflux; (c) Appropriate 1-bromo-2-nitrobenzene derivative, $Pd_2dba_3.CHCl_3$ (5 mol%), XPhos (10 mol%), Li*O*t*Bu, dry dioxane, 110 °C overnight, after filtration on Celite and evaporation, compounds were subject to Codagan cyclization; (d) $MoO_2Cl_2(dmf)_2$ (10 mol %), PPh_3 (4 equiv), in 3 mL of dioxane under microwave irradiation (MWI) at 135 °C; (e) NaH, CH_3I, DMF, rt.

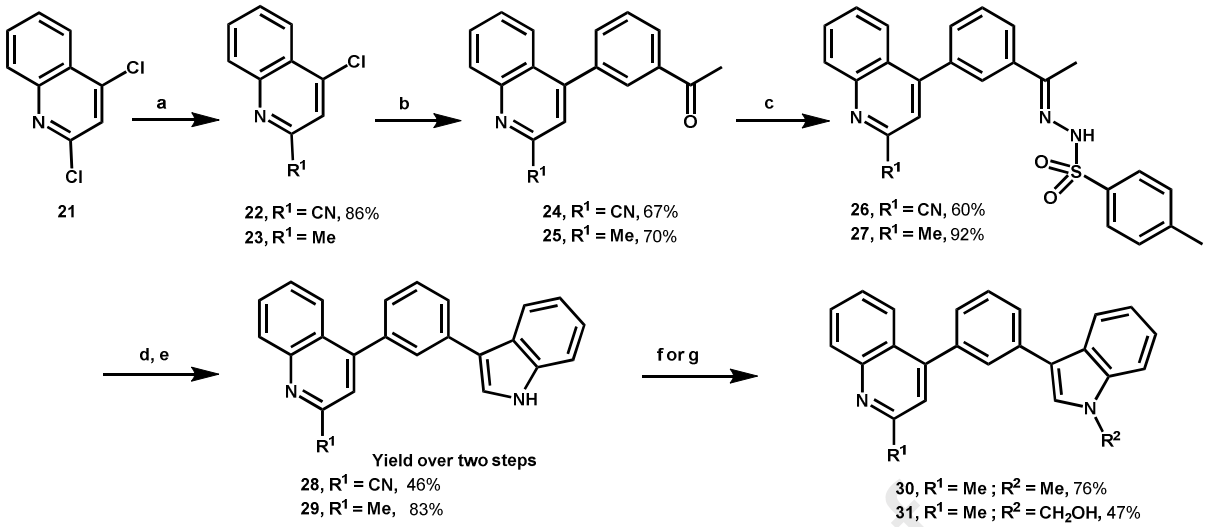

Scheme 2. (a) $Pd(PPh_3)_4$, $Zn(CN)_2$, DMF, 120 °C; (b) 3-acetylphenyl)boronic acid, $Pd(PPh_3)_4$, $K_3PO_4.H_2O$, Dioxane/H_2O, 110 °C; (c) 4-methylbenzenesulfonohydrazide, EtOH, 95 °C; (d) 1-bromo-2-nitrobenzene $Pd_2dba_3.CHCl_3$ (5 mol%), XPhos (10 mol%), Li*O*t*Bu*, dry dioxane, 110 °C overnight, after filtration on Celite and evaporation, the crude was subject to Codagan cyclization; (e) $MoO_2Cl_2(dmf)_2$ (10 mol %), PPh_3 (4 equiv),), in 3 mL of dioxane under MWI at 135 °C; (f): NaH, CH_3I, DMF, rt; (g): $NaOH_{aq}$, $HCOH_{aq}$, EtOH, rt.

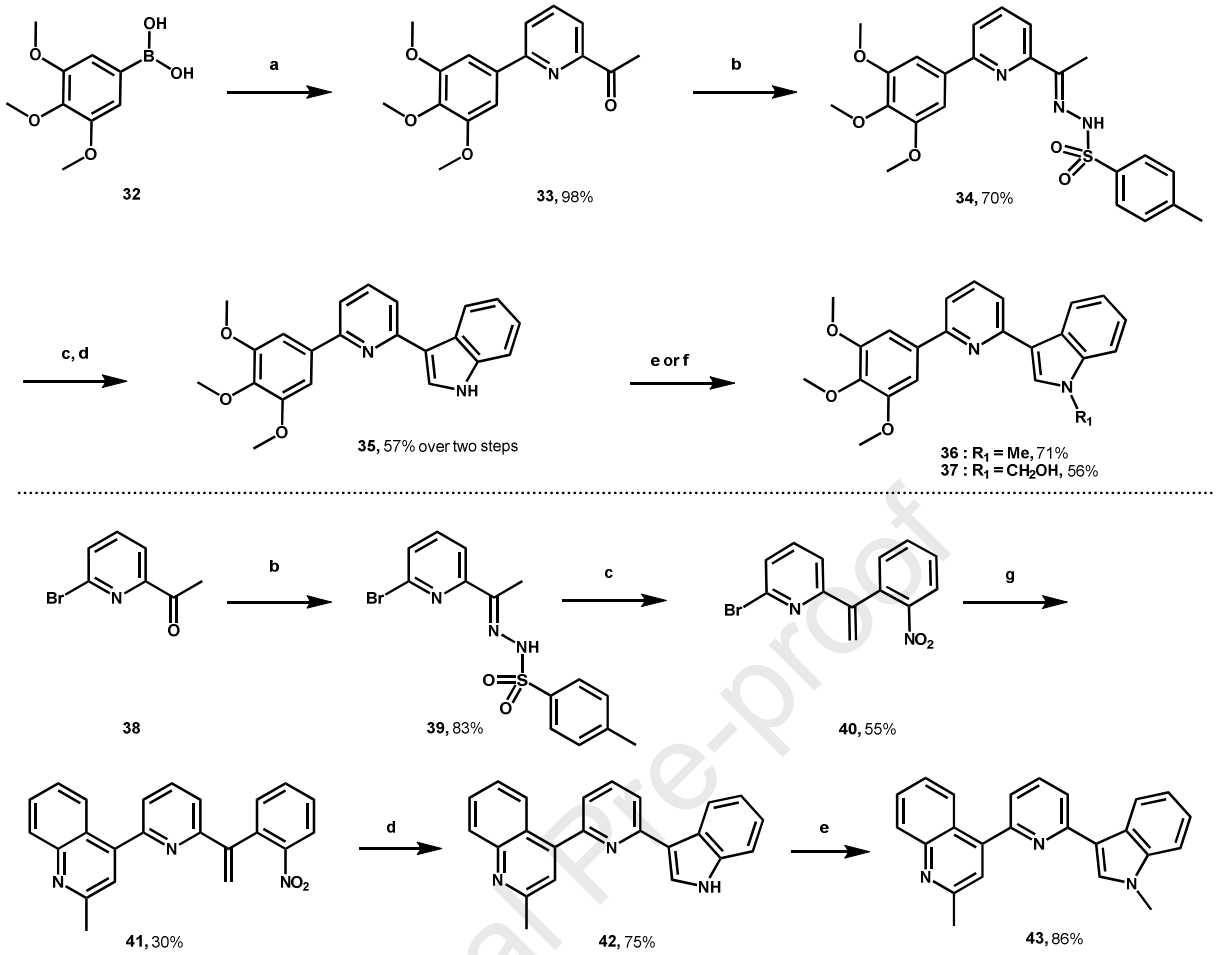

Scheme 3. (a) 3,4,5-trimethoxyphenylboronic acid, 1-(6-bromopyridin-2-yl)ethanone, $Pd(OAc)_2$, PPh_3, K_2CO_3, dioxane/H_2O, 110 °C, overnight; (b) (4-methylbenzenesulfonohydrazide, EtOH, 95 °C; (c) 1-iodo-2-nitrobenzene, $Pd_2dba_3.CHCl_3$ (5 mol%), XPhos (10 mol%), LiO*t*Bu, dry dioxane, 100 °C overnight; (d) $MoO_2Cl_2(dmf)_2$ (10 mol %), PPh_3 (4 equiv), in 3 mL of dioxane under MWI at 135 °C; (e) NaH, CH_3I, DMF, rt; (f) (33), $NaOH_{aq}$, $HCOH_{aq}$, EtOH, rt; (g) 2-methylquinolin-4-yl)boronic acid, $Pd_2dba_3.CHCl_3$, SPhos, K_2CO_3, 100 °C.

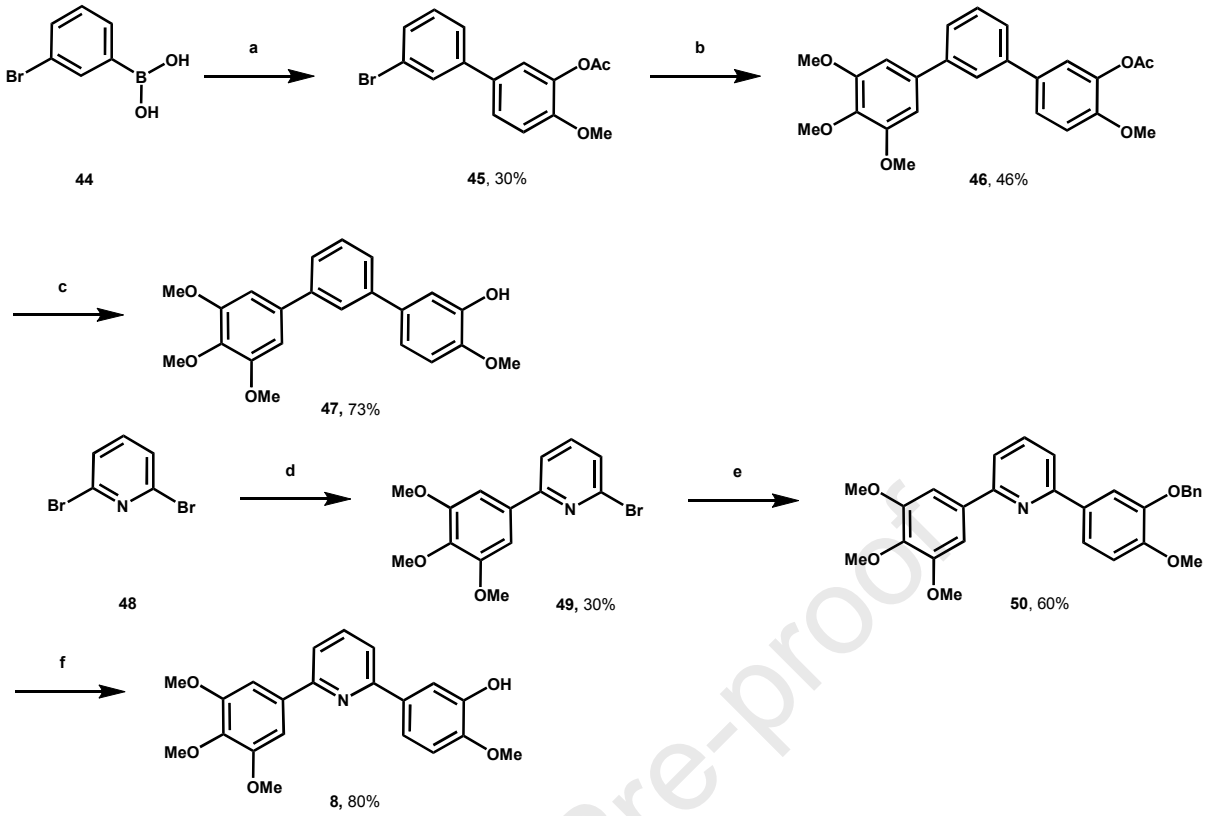

44

45, 30%

46, 46%

47, 73%

48

49, 30%

50, 60%

8, 80%

Scheme 4. (a) 5-iodo-2-methoxyphenyl acetate, $Pd(PPh_3)_4$ (2 mol%), K_2CO_3,Toluene/H_2O (4:1), 110 °C, 1 h; (b) (3,4,5-trimethoxyphenyl)boronic acid, $Pd(PPh_3)_4$ (2 mol%), K_2CO_3, Toluene/H_2O (4:1), 110 °C, 1 h; (c) K_2CO_3 (10 eq), MeOH, 50 °C, overnight; (d) (3,4,5-trimethoxyphenyl)boronic acid, $Pd(OAc)_2$ (5 mol%), $P(Cy_3).BF_4$ (10 mol%), K_2CO_3, Toluene/H_2O (30:1), 110 °C, 20 min; (e) (3-(benzyloxy)-4-methoxyphenyl)boronic acid, $Pd(OAc)_2$ (5 mol%), PPh_3 (10 mol%), K_2CO_3, Dioxane/H_2O (2:1), 110 °C, 1 h; (f) Pd/C H_2, (10 mol%), EtOH, rt, overnight.

Highlights

- Quinaldinyl-Pyridyl-Indole (QnPyInd) was discovered as novel tubulin inhibitors.
- Compound **42** displayed excellent antiproliferative activity with average IC_{50} of 5.6 nM.
- **42** exhibited high antiproliferative activity against resistant K562R and HT-29 cell lines.
- **42** inhibited tubulin polymerization both in vitro and in cells and induced G2/M cell cycle arrest.
- The safety profile of **42** was demonstrated in human no cancer cells PBLs.

Declaration of interests

☒ The authors declare that they have no known competing financial interests or personal relationships that could have appeared to influence the work reported in this paper.

☐The authors declare the following financial interests/personal relationships which may be considered as potential competing interests: